Kodaikanal Obs. Bull. (1986) 5, 155 - 200

LINE PROFILES IN AN EXPANDING SPHERICAL MEDIUM

A. PERAIAH, M SRINIVASA RAO AND B.A. VARGHESE

ABSTRACT

We have applied the discrete space theory of radiative transfer with the integral operator technique to calculate the spectral line profiles formed in a spherically symmetric expanding stellar atmospheres. We calculated the source function in the comoving frame and this is employed to simulate the line profiles observed at infinity We have considered line absorption, emission and velocities of expansion in a parametrised form Complete redistribution of photons in the line in a two level atom is assumed with a Doppler profiles function. In all cases we have employed the equation of continuity (i.e.) $4\pi r^2 \rho V$ = constant (where ρ and V are the density and velocity respectively at r) as a guide line for determining the density and the velocity of expansion. Many P Cygni type profiles are obtained. This is true particularly when velocity gradients are present in the medium. The results are similar to those of Beals (1950).

Key Words : comoving frame, radiative transfer in spherical symmetry, P-Cygni type profiles, velocity gradients

1. Introduction

It is well known that gases in the outer layers of many O-B supergiants, Wolf-Rayet stars, P Cygni type stars, quasars, novae, nuclei of Seyfert galaxies show evidence of radial expansion. Simulation of spectral lines formed in such media is a matter of some difficulty. This is because of the fact that the photons are redistributed after each absorption and emission. The radiation leaves the medium through two ways (1) by velocity gradients and (2) by the wing photons. The effects of velocity gradients on the wing photons, and on photon redistribution in the line are quite difficult to estimate. In a medium which is in motion, the line photons can be redistributed in the interval $\nu\,(1 - \frac{V_{max}}{C})$ to $\nu\,(1 + \frac{V_{max}}{C})$ where ν is the frequency of the photons at the line centre and V_{max} is the gas velocity and C is the velocity of light. There were several attempts to simulate lines in expanding media in recent years (Hummer and Kunasz 1974, Peraiah 1978, Peraiah and Wehrse 1978, Wehrse and Peraiah 1979) But these were done in the rest frame of the star and therefore were good only upto a maximum of 2 to 3 mean thermal units (mtu). If one wants to calculate the radiation field in the rest frame we have to extend the frequency mesh to the interval of $\nu\,(1 \pm \frac{V_{max}}{C})$. This becomes quite unmanageable because V_{max} is nearly 100 mtu in some stars. This difficulty is avoided in a comoving frame in which the observer need not take into account the Doppler shifts directly that enter into the absorption co-

efficient in the rest frame calculation. Calculation of photon redistribution becomes easy in the comoving frame.

Simmonneau (1973), Mihalas et al. (1975), Peraiah (1980a, b; 1984) have made several attempts to calculate solution of line transfer in comoving frame. However these techniques suffer from several difficulties such as iteration which is time consuming or too complicated to understand at first sight.

In an earlier paper (Peraiah and Varghese 1985, henceforth called paper 1), we presented a method of obtaining numerical solution of radiative transfer equation in spherical symmetry. In this method we express the specific intensity in terms of certain interpolation coefficients, which in turn are expressed in terms of the nodal values of the angle-radius discrete grid. The transfer equation is then integrated on such a grid. In paper I, we presented a few useful checks on the stability of the solution and its applicability to different problems we encounter in stellar atmospheres by employing monochromatic radiation field. In this paper, we intend to extend the method given in paper I to polychromatic problems such as line formation in extended and expanding spherically symmetric media.

In Section II we present the method of obtaining solution in a comoving frame and in Section III, its applications are presented.

2. Integration of the Equation of Line Transfer in the Comoving Frame

We shall express the specific intensity in terms of certain interpolation coefficients and weights corresponding to radius, angle and frequency. These are given by

$$\xi = \frac{r - \bar{r}}{\Delta r/2}, \quad \eta = \frac{\mu - \bar{\mu}}{\Delta\mu/2} \quad \text{and} \quad \chi = \frac{x - \bar{x}}{\Delta x/2} \tag{1}$$

where r is the radius, μ is the cosine of the angle made by the ray with the radius vector at the radial point r and x is given by

$$x = \frac{\nu - \nu_0}{\Delta_s} \tag{2}$$

where ν_0 and ν are the frequencies at the centre and at any other point in the line. And Δ_s is some standard frequency interval. Further more (see Fig.1)

$$\bar{r} = \tfrac{1}{2}(r_i + r_{i-1}), \quad \Delta r = (r_i - r_{i-1}) \tag{3}$$

$$\bar{\mu} = \tfrac{1}{2}(\mu_j + \mu_{j-1}), \quad \Delta\mu = (\mu_j - \mu_{j-1}) \tag{4}$$

$$\bar{x} = \tfrac{1}{2}(x_k + x_{k-1}), \quad \Delta x = (x_k - x_{k-1}) \tag{5}$$

We shall write that

$$U(r, \mu, x) = 4\pi r^2 I(r, \mu, x) \tag{6}$$

where $I(r, \mu, x)$ is the specific intensity.

In terms of quantities defined in equations (1) to (5) the specific intensity is written as,

$$U(r, \mu, x) = U_o + U_r\xi + U_\mu\eta + U_x\chi + U_{r\mu}\xi\eta + U_{\mu x}\eta\chi + U_{xr}\chi\xi + U_{r\mu}\xi\eta\chi \tag{7}$$

where U_o, U_r, U_μ, U_x, $U_{r\mu}$, $U_{\mu x}$, U_{xr} and $U_{r\mu x}$ are the interpolation coefficients. The nodal values can be expressed in terms of the interpolation coefficients and are given below (see Figure 1):

$$U(r_{i-1}, \mu_{j-1}, X_{k-1}) = U_o - U_r - U_\mu - U_x + U_{r\mu} + U_{\mu x} + U_{xr} - U_{r\mu x} = U_a \tag{8}$$

$$U(r_{i-1}, \mu_j, X_{k-1}) = U_o - U_r + U_\mu - U_x - U_{r\mu} - U_{\mu x} + U_{xr} - U_{r\mu x} = U_b \tag{9}$$

$$U(r_{i-1}, \mu_j, X_k) = U_o - U_r + U_\mu + U_x - U_{r\mu} + U_{\mu x} - U_{xr} - U_{r\mu x} = U_c \tag{10}$$

$$U(r_{i-1}, \mu_{j-1}, X_k) = U_o - U_r - U_\mu + U_x + U_{r\mu} - U_{\mu x} - U_{xr} + U_{r\mu x} = U_d \tag{11}$$

$$U(r_i, \mu_{j-1}, X_k) = U_o + U_r - U_\mu + U_x - U_{r\mu} - U_{\mu x} + U_{xr} - U_{r\mu x} = U_e \tag{12}$$

$$U(r_i, \mu_{j-1}, X_{k-1}) = U_o + U_r - U_\mu - U_x - U_{r\mu} + U_{\mu x} - U_{xr} + U_{r\mu x} = U_f \tag{13}$$

$$U(r_i, \mu_j, X_{k-1}) = U_o + U_r + U_\mu - U_x + U_{r\mu} - U_{\mu x} - U_{xr} - U_{r\mu x} = U_g \tag{14}$$

$$U(r_i, \mu_j, X_k) = U_o + U_r + U_\mu - U_x + U_{r\mu} + U_{\mu x} + U_{xr} + U_{r\mu x} = U_h \tag{15}$$

The interpolation coefficients U_o, U_r, U_μ etc., are obtained from equations (8) to (15). These are given by,

$$U_o = \frac{1}{8}[U_a + U_b + U_c + U_d + U_e + U_f + U_g + U_h] \tag{16}$$

$$U_r = \frac{1}{8}[-U_a - U_b - U_c - U_d + U_e + U_f + U_g + U_h] \tag{17}$$

$$U_\mu = \frac{1}{8}[-U_a + U_b + U_c - U_d - U_e - U_f + U_g + U_h] \tag{18}$$

$$U_x = \frac{1}{8}[-U_a - U_b + U_c + U_d + U_e - U_f - U_g + U_h] \tag{19}$$

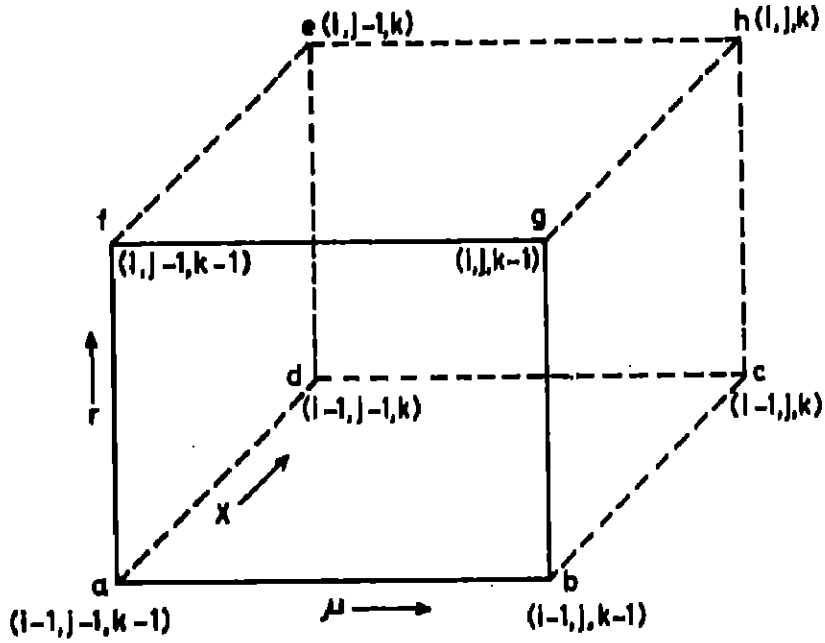

Fig.1 Schematic diagram of angle - radius - frequency grid.

$$U_{r\mu} = \frac{1}{8}[U_a - U_b - U_c + U_d - U_e - U_f + U_g + U_h] \quad (20)$$

$$U_{\mu x} = \frac{1}{8}[U_a + U_b - U_c - U_d + U_e - U_f - U_g + U_h] \quad (21)$$

$$U_{xr} = \frac{1}{8}[U_a + U_b - U_c - U_d + U_e - U_f - U_g + U_h] \quad (22)$$

$$U_{r\mu x} = \frac{1}{8}[-U_a + U_b - U_c + U_d - U_e + U_f - U_g + U_h] \quad (23)$$

The equation of line transfer in a comoving frame can be written as (Mihalas, et al. 1975):

$$\mu \frac{\partial U(r, \mu, x)}{\partial r} + \frac{1}{r}\frac{\partial}{\partial \mu}\{(1-\mu^2)U(r, \mu, x)\} = K_L(\beta + \phi(r, \mu, x))$$

$$[S(r, \mu, x) - U(r, \mu, x)] + [(1-\mu^2)\frac{V'(r)}{r} + \mu^2\frac{dV'(r)}{dr}]\frac{\partial U(r, \mu, x)}{\partial x} \quad (24)$$

for the oppositely directed beam,

$$-\mu \frac{\partial U(r, -\mu, x)}{\partial r} - \frac{1}{r}\frac{\partial}{\partial \mu}\{(1-\mu^2)U(r, -\mu, x)\} = K_L(\beta + \phi(r, -\mu, x))$$

$$[S(r, -\mu, x) - U(r, -\mu, x)] + [(1-\mu^2)\frac{V'(r)}{r} + \mu^2\frac{dV'(r)}{dr}]\frac{\partial U(r, -\mu, x)}{\partial x} \quad (25)$$

where $V'(r)$ is the velocity of the gas in mean thermal units at r and $S(r, \mu, x)$ is the source function given by

$$S(r, \mu, x) = \frac{\phi(r, \mu, x)}{\beta + \phi(r, \mu, x)} S_L(r) + \frac{\beta}{\beta + \phi(r, \mu, x)} S_C(r, \mu, x) \quad (26)$$

where S_L (r) and S_c(r, μ, x) are the line and continuum source functions respectively and they are given by

$$S_c\ (r,\ \mu,\ x) = \rho(r)\ B\ (\nu_o,\ T_o(r)) \tag{27}$$

$$S_L\ (r) = (1-\varepsilon)\ \int_{-\infty}^{+\infty} \phi\ (x)\ J_x\ dx + \varepsilon B(r) \tag{28}$$

where $\phi(x)$ is the profile function and J_x is the mean intensity at frequency x

Here $\rho(r)$ is a certain function of r to be specified later, B (ν_o, T_o (r)) is the Planck function with frequency ν_o and temperature T_o The quantity ε is the probability per scatter that a photon will be destroyed by collisional de-excitation and β is the ratio of continuum to line absorption coefficients per unit frequency interval

The source function can be expressed in terms of interpolation coefficients similar to those given in equation (7) This is given by,

$$S(r,\ \mu,\ x) = S_o + S_r\xi + S_\mu\eta + S_x\chi + S_{r\mu}\xi\eta + S_{\mu x}\eta + S_{xr}\chi\xi + S_{r\mu x}\xi\eta\chi \tag{29}$$

where S_o, S_r, S_μ etc, are the interpolation co-efficients By substituting equations (7) and (29) into (24), we obtain,

$$\begin{aligned}
&\frac{2\mu}{\Delta r}\ (U_r + U_{r\mu}\eta + U_{xr}\chi + U_{r\mu x}\eta\chi)\ -\ \frac{2\mu}{r}\ (U_o + U_r\xi + U_\mu\eta + U_x\chi \\
&\quad + U_{r\mu}\xi\eta + U_{\mu x}\eta\chi + U_{xr}\chi\xi + U_{r\mu x}\xi\eta\chi) \\
&\quad + \frac{1-\mu^2}{r}\frac{2}{\Delta\mu}\ (U_\mu + U_{r\mu}\xi + U_{\mu x}\chi + U_{r\mu x}\xi\chi) \\
&\quad = K\ \{(S_o + S_r\xi + S_\mu\eta + S_x\chi + S_{r\mu}\xi\eta + S_{\mu x}\eta\chi \\
&\quad + S_{xr}\chi\xi + S_{r\mu x}\xi\eta\chi) - (U_o + U_r\xi + U_\mu\eta + U_x\chi \\
&\quad + U_{r\mu}\xi\eta + U_{\mu x}\eta\chi + U_{xr}\chi\xi + U_{r\mu x}\xi\eta\chi) \\
&+ \frac{2}{\Delta x}\ \{(1-\mu^2)\ \frac{V'(r)}{r} + \mu^2\frac{dV'(r)}{dr}\}(U_x + U_{\mu x}\eta + U_{xr}\xi + U_{r\mu x}\xi\eta)
\end{aligned} \tag{30}$$

We shall employ the following integrals given by (31)

$$\theta_\mu = \frac{1}{\Delta\mu}\int_{\Delta\mu} \qquad d\mu \text{ (for angle integration)} \tag{32}$$

$$\theta_V = \frac{1}{V}\int_{\Delta r} \qquad 4\pi r^2\, dr \text{ (for radial integration)}$$

$$\theta_x = \frac{1}{x} \int_{\Delta x} \ldots dx \text{ (for frequency integration)} \tag{33}$$

We shall now apply θ_μ on equation (30) and obtain,

$$\begin{aligned}
&\frac{2}{\Delta r}\{\bar{\mu}(U_r + U_{xr}\chi) + \frac{1}{6}\Delta\mu\,(U_{r\mu} + U_{r\mu x}\chi)\} \\
&+ \frac{2}{r}\frac{1}{\Delta\mu}(1-\bar{\mu}^2)(U_\mu + U_{r\mu}\xi + U_{\mu x}\xi + U_{r\mu x}\xi\chi) \\
&- \frac{2\bar{\mu}}{r}(U_o + U_r\xi + U_x\chi + U_{xr}\chi\xi) \\
&- \frac{1}{3}\frac{\Delta\mu}{r}(U_\mu + U_{r\mu}\xi + U_{\mu x}\chi + U_{r\mu x}\xi\chi) \\
= K\{&(S_o + S_r\xi + S_x\chi + S_{xr}\chi\xi) - (U_o + U_r\xi + U_x\chi + U_{xr}\xi\chi)\} \\
&+ \frac{2}{\Delta x}[(U_x + U_{xr}\xi)\{(1-\mu^2)\frac{V'(r)}{dr}\} \\
&+ \bar{\mu}^2\frac{dV'(r)}{dr} + \frac{1}{3}\bar{\mu}\Delta\mu(U_{\mu x} + U_{r\mu x}\xi)\{\frac{dV'(r)}{dr} - \frac{V'(r)}{r}\}]
\end{aligned} \tag{34}$$

Applying θ_V on equation (34), we obtain,

$$\begin{aligned}
&\frac{2}{\Delta r}\{\bar{\mu}(U_r + U_{xr}\chi) + \frac{1}{6}\Delta\mu\,(U_{r\mu} + U_{r\mu x}\chi)\} \\
&+ \frac{2}{\Delta\mu}(1-\bar{\mu}^2)\{(U_\mu + U_{\mu x}\chi)\frac{1}{2}\frac{\Delta A}{V} + \frac{1}{\Delta r}(2-\frac{\bar{r}\Delta A}{V}) \\
&(U_{r\mu} + U_{r\mu x}\chi)\} \\
&- 2\bar{\mu}\{\frac{1}{2}(U_o + U_x\chi)\frac{\Delta A}{V} + \frac{1}{\Delta r}(2-\bar{r}\frac{\Delta A}{V})(U_r + U_{xr}\chi)\}, \\
&- \frac{1}{3}\Delta\mu\{\frac{1}{2}(U_\mu + U_{\mu x}\chi)\frac{\Delta A}{V} + \frac{1}{\Delta r}(2-\bar{r}\frac{\Delta A}{V})(U_{r\mu} + U_{r\mu x}\chi)\} \\
= K[&\{(S_o + S_x\chi) + \frac{1}{6}(S_r + S_{xr}\chi)\frac{\Delta A}{\bar{A}} - (U_o + U_x\chi) + \frac{1}{6}(U_r + U_{xr}\chi)\frac{\Delta A}{\bar{A}}\}] \\
&+ \frac{2}{\Delta x}[(1-\bar{\mu}^2)V'\{\frac{1}{2}U_x\frac{\Delta A}{V} + \frac{1}{\Delta r}(2-\bar{r}\frac{\Delta A}{V})U_{xr}\} \\
&+ \bar{\mu}^2\frac{dV'}{dr}(U_x + \frac{1}{6}U_{xr}\frac{\Delta A}{\bar{A}}) + \frac{1}{3}\Delta\mu\cdot\bar{\mu}\frac{dV'}{dr}(U_{\mu x} + \frac{1}{6}U_{r\mu x}\frac{\Delta A}{\bar{A}}) \\
&- \frac{1}{3}V'\Delta\mu\cdot\bar{\mu}\{\frac{1}{2}\frac{\Delta A}{V}U_{\mu x} + \frac{1}{\Delta r}(2-\bar{r}\frac{\Delta A}{V})U_{r\mu x}]
\end{aligned} \tag{35}$$

we shall apply the operator θ_x on equation (35) and obtain

$$\frac{2}{\Delta r}\left(\bar{\mu}U_r + \frac{1}{6}\Delta\mu\, U_{r\mu}\right) + \frac{2}{\Delta\mu}(1-\bar{\mu}^2)\left\{\frac{1}{2}\frac{\Delta A}{V}U_\mu + \frac{1}{\Delta r}\left(2-\bar{r}\frac{\Delta A}{V}\right)U_{r\mu}\right\} - 2\bar{\mu}\left\{\frac{1}{2}\frac{\Delta A}{V}U_o + \frac{1}{\Delta r}\left(2\,r\frac{\Delta A}{V}\right)U_r\right\} - \frac{1}{3}\Delta\mu\left\{\frac{1}{2}\frac{\Delta A}{V}U_\mu + \frac{1}{\Delta r}\left(2-\bar{r}\frac{\Delta A}{V}\right)U_{r\mu}\right\}$$

$$= K\left\{\left(S_o + \frac{1}{6}\frac{\Delta A}{\bar{A}}S_r\right) - \left(U_o + \frac{1}{6}\frac{\Delta A}{\bar{A}}U_r\right)\right\}$$

$$+ \frac{2}{\Delta x}\left[\left\{\frac{1}{2}V'\frac{\Delta A}{V}(1-\bar{\mu}^2) + \bar{\mu}^2\frac{dV'}{dr}\right\}U_x + \left\{\frac{V'}{\Delta r}\left(2-\bar{r}\frac{\Delta A}{V}\right)(1-\mu^2) + \frac{1}{6}\frac{\Delta A}{\bar{A}}\bar{\mu}^2\frac{dV'}{dr}\right\}U_{xr} + \left\{\frac{1}{3}\Delta\mu\,\bar{\mu}\frac{dV'}{dr} - \frac{1}{6}V'\Delta\mu\,\bar{\mu}\frac{\Delta A}{V}\right\}U_{\mu x} + \left\{\frac{1}{18}\Delta\mu\,\bar{\mu}\frac{dV'}{dr}\frac{\Delta A}{\bar{A}} - \frac{1}{3}\frac{1}{\Delta r}V'\Delta\mu\,\bar{\mu}\left(2-\bar{r}\frac{\Delta A}{V}\right)\right\}U_{r\mu x}\right] \tag{36}$$

where

$$\bar{\mu}^2 = (\bar{\mu})^2 + \frac{(\Delta\mu)^2}{12}$$

$$V = \frac{4}{3}\pi\left(r_l^3 - r_{l-1}^3\right) \tag{37}$$

$$\Delta A = 4\pi\left(r_l^2 - r_{l-1}^2\right) \tag{38}$$

$$\bar{A} = V/\Delta r \tag{39}$$

We substitute equations (7) and (29) into equation (25) and then apply the integral operators θ_μ, θ_V and θ_X successively and obtain,

$$-\frac{2}{\Delta r}\left(\bar{\mu}U_r + \frac{1}{6}\Delta\mu U_{r\mu}\right) - \frac{2}{\Delta\mu}(1-\bar{\mu}^2)\left\{\frac{1}{2}\frac{\Delta A}{V}U_\mu + \frac{1}{\Delta r}\left(2-\bar{r}\frac{\Delta A}{V}\right)U_{r\mu}\right\} + 2\bar{\mu}\left\{\frac{1}{2}\frac{\Delta A}{V}U_o + \frac{1}{\Delta r}\left(2-\bar{r}\frac{\Delta A}{V}\right)U_r\right\} + \frac{1}{3}\Delta\mu\left\{\frac{1}{2}\frac{\Delta A}{V}U_\mu + \frac{1}{\Delta r}\left(2-\bar{r}\frac{\Delta A}{V}\right)U_{r\mu}\right\} = K\left\{\left(S_o + \frac{1}{6}\frac{\Delta A}{\bar{A}}S_r\right) - \left(U_o + \frac{1}{6}\frac{\Delta A}{\bar{A}}U_r\right)\right\} + U_x\left\{\frac{2}{\Delta x}\left[\frac{1}{2}(1-\bar{\mu}^2)V'\frac{\Delta A}{V} + \bar{\mu}^2\frac{dV'}{dr}\right]\right\}$$

$$+ U_{xr} \left\{ \frac{2}{\Delta x} \left[\frac{V'}{\Delta r} (1-\bar{\mu}^2)(2-\bar{r}\frac{\Delta A}{V}) + \frac{1}{6}\bar{\mu}^2 \frac{dV'}{dr} \cdot \frac{\Delta A}{\bar{A}} \right] \right\}$$

$$+ U_{\mu x} \left\{ \frac{2}{\Delta x} \left[\frac{1}{3} \Delta\mu . \bar{\mu} \frac{dV'}{dr} - \frac{1}{6} V' \Delta\mu . \bar{\mu} \frac{\Delta A}{V} \right] \right\}$$

$$+ U_{r\mu x} \left\{ \frac{2}{\Delta x} \left[\frac{1}{18} \Delta\mu . \bar{\mu} \frac{dV'}{dr} \frac{\Delta A}{\bar{A}} - \frac{1}{3} \frac{\Delta\mu . \bar{\mu}}{\Delta r} V' (2-\bar{r}\frac{\Delta A}{V}) \right] \right\} \quad (40)$$

We replace the interpolation coefficients U_o, U_r, U_μ etc and S_o, S_r, S_μ etc in equations (36) and (40) by the nodal values U_a, U_b, ..., U_h and S_a, S_b, ... S_h given in equations (16) to (23).

Equations (36) and (40) will thus be written as,

$$A_a U_a^+ + A_b U_b^+ + A_c U_c^+ + A_d U_d^+ + A_e U_e^+ + A_f U_f^+ + A_g U_g^+ + A_h U_h^+$$

$$= \tau^-(S_a^+ + S_b^+ + S_c^+ + S_d^+) + \tau^+(S_e^+ + S_f^+ + S_g^+ + S_h^+) \quad (41)$$

and

$$A_a U_a^- + A_b U_b^- + A_c U_c^- + A_d U_d^- + A_e U_e^- + A_f U_f^- + A_g U_g^- + A_h U_h^-$$

$$= \tau^-(S_a^- + S_b^- + S_c^- + S_d^-) - \tau^-(S_e^- + S_f^- + S_g^- + S_h^-) \quad (42)$$

where

$$\tau^+ = \tau(1 + \frac{1}{6}\frac{\Delta A}{\bar{A}}) \quad (43)$$

$$\tau^- = \tau(1 - \frac{1}{6}\frac{\Delta A}{\bar{A}}) \quad (44)$$

$$\tau = K\Delta r \quad (45)$$

U_a^+, U_b^+ etc. and U_a^-, U_b^- etc. represent the intensities of the beams of radiation in the opposite directions. The quantities A_a, A_b etc. are given in the Appendices I and II.

We shall now make the substitutions that (see Figure 1)

$$U_a^+ = U_{j-1,k-1}^{l-1,+},\ U_b^+ = U_{j,k-1}^{l-1,+},\ U_c^+ = U_{j,k}^{l-1,+},\ U_d^+ = U_{j-1,k}^{l-1,+} \quad (46)$$

$$U_e^+ = U_{j-1,k}^{l,+},\ U_f^+ = U_{j-1,k-1}^{l,+},\ U_g^+ = U_{j,k-1}^{l,+},\ U_h^+ = U_{j,k}^{l,+}$$

together with similar equations for U_a^-, U_b^- etc and $S_a^{\pm}$, $S_b^{\pm}$ etc into equations (41) and obtain for $(j-1)^{th}$ and j^{th} angles

$$A^a_{j-1}\, U^{i-1,+}_{j-1,k-1} + A^b_j\, U^{i-1,+}_{j,k-1} + A^c_j\, U^{i-1,+}_{j,k} + A^d_{j-1}\, U^{i-1,+}_{j-1,k}$$

$$+ A^e_{j-1}\, U^{i,+}_{j-1,k} + A^f_{j-1}\, U^{i,+}_{j-1,k-1} + A^g_j\, U^{i,+}_{j,k-1} + A^h_j\, U^{i,+}_{j,k}$$

$$\tau^- \{[\sigma\phi^{i-1,+}_{j-1,k-1} \sum_{k'=-K}^{K} a_{k'}\, \phi^{i-1}_{k'} \sum_{j'=1}^{J} C_{j'}\, (U^{i-1,+}_{j',k-} + U^{i-1,-}_{j',k-1})]$$

$$+ (\varepsilon\, \phi^{i-1,+}_{j-1,k-1} + \rho\beta) B^{i-1,+}_{j-1,k-1}$$

$$+ [\sigma\phi^{i-1,+}_{j,k-1} \sum_{k'=-K}^{K} a_{k'}\, \phi^{i-1}_{k'} \sum_{j'=1}^{J} C_{j'}\, (U^{i-1,+}_{j',k-1} + U^{i-1,-}_{j',k-1})]$$

$$+ (\varepsilon\, \phi^{i-1,+}_{j,k-1} + \rho\beta) B^{i-1,+}_{j,k-1}$$

$$+ [\sigma\phi^{i-1,+}_{j-1,k} \sum_{k'=-K}^{K} a_{k'}\, \phi^{i-1}_{k'} \sum_{j'=1}^{J} C_{j'}\, (U^{i-1,+}_{j',k} + U^{i-1,-}_{j',k})]$$

$$+ (\varepsilon\phi^{i-1,+}_{j-1,k} + \rho\beta) B^{i-1,+}_{j-1,k}$$

$$+ [\sigma\phi^{i-1,+}_{j,k} \sum_{k'=-K}^{K} a_{k'}\, \phi^{i-1}_{k'} \sum_{j'=1}^{J} C_{j'}\, (U^{i-1,+}_{j',k} + U^{i-1,-}_{j',k})]$$

$$+ (\varepsilon\phi^{i-1,+}_{j,k} + \rho\beta) B^{i-1,+}_{j,k}\}$$

$$+ \tau^+ \{[\sigma\phi^{i,+}_{j-1,k} \sum_{k'=-K}^{K} a_{k'}\, \phi^{i}_{k'} \sum_{j'=1}^{J} C_{j'}\, (U^{i,+}_{j',k} + U^{i,-}_{j',k})]$$

$$+ (\varepsilon\phi^{i,+}_{j-1,k} + \rho\beta) B^{i,+}_{j-1,k}$$

$$+ [\sigma\phi^{i,+}_{j,k-1} \sum_{k'=-K}^{K} a_{k'}\, \phi^{i}_{k'} \sum_{j'=1}^{J} C_{j'}\, (U^{i,+}_{j',k-1} + U^{i,-}_{j',k})]$$

$$+ (\varepsilon\phi^{i,+}_{j,k-1} + \rho\beta) B^{i,+}_{j,k-1}$$

$$+ [\sigma\phi^{i,+}_{j-1,k-1} \sum_{k'=-K}^{K} a_{k'}\, \phi^{i}_{k'} \sum_{j'=1}^{J} C_{j'}\, (U^{i,+}_{j',k+1} + U^{i,-}_{j',k-1})]$$

$$+ (\varepsilon\phi^{l,+}_{j-1,k-1} + \rho\beta)B^{i,+}_{j-1,k-1}$$

$$+ [\sigma\phi^{i,+}_{j,k} \sum_{k'=-K}^{K} a_{k'}\, \phi^{l}_{k'} \sum_{j'=1}^{J} C_{j'}\, (U^{l,+}_{j',k} + U^{l,-}_{j',k})]$$

$$+ (\varepsilon\phi^{l,+}_{j,k} + \rho\beta)B^{i,+}_{j,k}] \tag{47}$$

where $\sigma = (1-\varepsilon)/2$ (48)

Similarly equation (42) is rewritten. Succintly we can rewrite equation (47) and the corresponding equation for the oppositely directed beam as follows:

$$(A^{ab}U^{l-1,+}_{k-1} - \tau^{-}\sigma Q\, \phi^{l-1,+}_{k-1}Y^{+}_{k-1}) + (A^{dc}U^{l-1,+}_{k} - \tau^{-}\sigma Q\phi^{i-1,+}_{k}Y^{+}_{k})$$

$$+ (A^{fg}U^{l,+}_{k-1} - \tau^{+}\sigma Q\phi^{l,+}_{k-1}Y^{+}_{k-1}) + (A^{eh}U^{l,+}_{k} - \tau^{+}\sigma Q\phi^{i,+}_{k}Y^{+}_{k})$$

$$= \tau^{-}\sigma Q(\phi^{l-1,+}_{k-1}Y^{-}_{k-1} + \phi^{i-1,+}_{k}Y^{-}_{k}) + \tau^{+}\sigma Q(\phi^{l,+}_{k-1}Y^{-}_{k-1} + \phi^{l,+}_{k}Y^{-}_{k})$$

$$+ \tau^{-}\sigma Q(\rho\beta + \varepsilon\phi^{l-1,+}_{k-1})B^{l-1,+}_{k-1} + \tau^{-}\sigma Q(\rho\beta + \varepsilon\phi^{l-1,+}_{k})B^{l-1,+}_{k}$$

$$+ \tau^{+}\sigma Q(\rho\beta + \varepsilon\phi^{l,+}_{k-1})B^{l,+}_{k-1} + \tau^{+}\sigma Q(\rho\beta + \varepsilon\phi^{l,+}_{k})B^{i,+}_{k} \tag{49}$$

and

$$(D^{ab}U^{l-1,-}_{k-1} - \tau^{-}\sigma Q\phi^{l-1,-}_{k-1}Y^{-}_{k-1}) + (D^{dc}U^{l-1,-}_{k} - \tau^{-}\sigma Q\phi^{l-1,-}_{k}Y^{-}_{k})$$

$$(D^{fg}U^{l,-}_{k-1} - \tau^{+}\sigma Q\phi^{l,-}_{k-1}Y^{-}_{k-1}) + (D^{eh}U^{l,-}_{k} - \tau^{+}\sigma Q\phi^{l,-}_{k}Y^{-}_{k})$$

$$= \tau^{-}\sigma Q(\phi^{l-1,-}_{k-1}Y^{+}_{k-1} + \phi^{l-1,-}_{k}Y^{+}_{k}) + \tau^{+}\sigma Q(\phi^{l,-}_{k-1}Y^{+}_{k-1} + \phi^{l,-}_{k}Y^{+}_{k})$$

$$+ \tau^{-}\sigma Q(\rho\beta + \varepsilon\phi^{l-1,-}_{k-1})B^{l-1,-}_{k-1} + \tau^{-}\sigma Q(\rho\beta + \varepsilon\phi^{l-1,-}_{k})B^{l-1,-}_{k}$$

$$+ \tau^{+}\sigma Q(\rho\beta + \varepsilon\phi^{l,-}_{k-1})B^{l,-}_{k-1} + \tau^{+}\sigma Q(\rho\beta + \varepsilon\phi^{l,-}_{k})B^{l,-}_{k} \tag{50}$$

where,

$$\mathbf{A}^{ab} = \begin{bmatrix} A^a_{j-1} & A^b_j & & \\ & A^a_j & A^b_{j+1} & \\ & & \ddots & \ddots \\ & & A^a_{J-1} & A^b_J \\ & & & A^a_J \end{bmatrix} \tag{51}$$

$$\mathbf{D}^{ab} = \begin{bmatrix} A'^a_{j-1} & A'^b_j & & \\ & A'^a_j & A'^b_{j+1} & \\ & & \ddots & \ddots \\ & & A'^a_{J-1} & A'^b_J \\ & & & A'^a_J \end{bmatrix} \tag{52}$$

$$\mathbf{Q} = \begin{bmatrix} 1 & 1 & & \\ & 1 & 1 & \\ & & \ddots & \ddots \\ & & 1 & 1 \\ & & & 1 \end{bmatrix} \tag{53}$$

for J angles (J rows and J coloumns)

$$\mathbf{U}^{i-1,+}_{k-1} = \begin{bmatrix} U(r_{i-1}, + \mu_{j-1}, X_{k-1}) \\ U(r_{i-1}, + \mu_j, X_{k-1}) \\ U(r_{i-1}, + \mu_J, X_{k-1}) \end{bmatrix} \tag{54}$$

$$Y_{k-1}^{l-1,\pm} = \sum_{k'=-K}^{K} a_{k'}\, \phi_{k'}^{l-1} \sum_{j'=1}^{J} C_{j'}\, U_{j',k-1}^{i-1,\pm} \tag{55}$$

The matrices A^{dc}, A^{fg}, A^{eh}, D^{dc}, D^{dg}, D^{eh} are expressed in a similar way as given in equations (51) and (52). Other factors are self explanatory.

$$A_q^{ab} = Q^{-1}A^{ab},\ A_q^{dc} = Q^{-1}A^{dc},\ A_q^{fg} = Q^{-1}A^{fg},\ A_q^{eh} = Q^{-1}A^{eh} \tag{56}$$

$$D_q^{ab} = Q^{-1}D^{ab},\ D_q^{dc} = Q^{-1}D^{dc},\ D_q^{fg} = Q^{-1}D^{fg},\ D_q^{eh} = Q^{-1}D^{eh} \tag{57}$$

and rewrite equations (40) and (50) as follows

$$\begin{aligned}
&(A_q^{ab}U_{k-1}^{l-1,+} - \tau^{-}\sigma\phi_{k-1}^{l-1,+}Y_{k-1}^{l-1,+}) + (A_q^{dc}U_k^{l-1,+} - \tau^{-}\sigma\phi_k^{l-1,+}Y_k^{l-1,+}) \\
&\quad + (A_q^{fg}U_{k-1}^{i,+} - \tau^{+}\sigma\phi_{k-1}^{i,+}Y_{k-1}^{i,+}) + (A_q^{eh}U_k^{i,+} - \tau^{+}\sigma\phi_k^{i,+}Y_k^{i,+}) \\
&= \tau^{-}\sigma(\phi_{k-1}^{l-1,+}Y_{k-1}^{l-1,-} + \phi_k^{l-1,+}Y_k^{l-1,-}) + \tau^{+}\sigma(\phi_{k-1}^{i,+}Y_{k-1}^{i,-} + \phi_k^{i,+}Y_k^{i,-}) \\
&\quad + \tau^{-}\sigma(\rho\beta + \varepsilon\phi_{k-1}^{l-1,+})B_{k-1}^{l-1,+} + \tau^{-}\sigma(\rho\beta + \varepsilon\phi_k^{l-1,+})B_k^{i-1,+} \\
&\quad + \tau^{+}\sigma(\rho\beta + \varepsilon\phi_{k-1}^{i,+})B_{k-1}^{i,+} + \tau^{+}\sigma(\rho\beta + \varepsilon\phi_k^{i,+})B_k^{i,+}
\end{aligned} \tag{58}$$

and

$$\begin{aligned}
&(D_q^{ab}U_{k-1}^{l-1,-} - \tau^{-}\sigma\phi_{k-1}^{l-1,-}Y_{k-1}^{l-1,-}) + (D_q^{dc}U_k^{l-1,-} - \tau^{-}\sigma\phi_k^{l-1,-}Y_k^{l-1,-}) \\
&\quad + (D_q^{fg}U_{k-1}^{l,-} - \tau^{+}\sigma\phi_{k-1}^{l,-}Y_{k-1}^{l,-}) + (D_q^{eh}U_k^{l,-} - \tau^{+}\sigma\phi_k^{l,-}Y_k^{l,-}) \\
&= \tau^{-}\sigma(\phi_{k-1}^{l-1,-}Y_{k-1}^{l-1,+} + \phi_k^{l-1,-}Y_k^{l-1,+}) + \tau^{+}\sigma(\phi_{k-1}^{l,-}Y_{k-1}^{l,+} + \phi_k^{l,-}Y_k^{l,+}) \\
&\quad + \tau^{+}\sigma(\rho\beta + \varepsilon\phi_{k-1}^{l-1,-})B_{k-1}^{l-1,-} + \tau^{-}\sigma(\rho\beta + \varepsilon\phi_k^{l-1,-})B_k^{l-1,-} \\
&\quad + \tau^{-}\sigma(\rho\beta + \varepsilon\phi_{k-1}^{l,-})B_{k-1}^{l,-} + \tau^{+}\sigma(\rho\beta + \varepsilon\phi_k^{l,-})B_k^{l,-}
\end{aligned} \tag{59}$$

We shall now write a set of equations for K(1≤k ≤ K) frequency points and write equations (58) and (59) as

$$(A^{ab}_{dc} - \sigma\tau^{-}F^{++}_{l-1})U^{+}_{l-1} + (A^{fg}_{eh} - \sigma\tau^{+}F^{++}_{l})U^{+}_{l}$$

$$= \sigma\tau^{-}F^{+-}_{l-1}U^{-}_{l-1} + \sigma\tau^{+}F^{+-}_{l}U^{-}_{l}$$

$$+ \sigma\tau^{-}\Phi^{+}_{l-1}B^{+}_{l-1} + \sigma\tau^{+}\Phi^{+}_{l}B^{+}_{l} \tag{60}$$

$$(\bar{D}^{ab}_{dc} - \sigma\tau^{-}F^{--}_{l-1})U^{-}_{l-1} + (\bar{D}^{fg}_{eh} - \sigma\tau^{+}F^{--}_{l})U^{-}_{l}$$

$$= \sigma\tau^{-}F^{-+}_{l-1}U^{+}_{l-1} + \sigma\tau^{+}F^{-+}_{l}U^{+}_{l} + \sigma\tau^{-}\Phi^{-}_{l-1}B^{-}_{l-1} + \sigma\tau^{+}_{l}\Phi^{-}_{l}B^{-}_{l} \tag{61}$$

where

$$A^{ab}_{dc} = Q_F^{-1} \quad A^{ab}_{dc} \tag{62}$$

with

$$Q_F = \begin{bmatrix} I & & & \\ & I & & \\ & & I & \\ & & & I \end{bmatrix} \tag{63}$$

where I is the identity matrix.

And

$$A^{ab}_{dc} = \begin{bmatrix} A^{ab}_{q,k-1} & A^{dc}_{q,k} & & \\ & A^{ab}_{q,k} & A^{dc}_{q,k+1} & \\ & & A^{ab}_{q,K-1} & A^{dc}_{q,K} \\ & & & A^{ab}_{q,K} \end{bmatrix} \tag{64}$$

$$\phi^{+}_{l-1}Y^{+}_{l-1} = [\phi_{+}\phi^{T}_{+}W^{++}]\ U^{+}_{l-1} = F^{++}_{l-1}U^{+}_{l-1} \tag{65}$$

$$\text{with} \quad W = [W_m\ \delta_{mm}] \tag{66}$$

$$W_m = a_k c_j,\ m = j+(k-1)J, \quad 1 \leq m \leq M = KJ$$

$$\phi^{+}_{l-1} = [\rho\beta + \epsilon\phi^{+}_{l-1}]\ \delta_{kk'} = [\phi_{kk}] \tag{67}$$

$$B^{+}_{l,l-1} = B^{+}_{l,l-1}\ L \tag{68}$$

$$L = [1 \quad 1 \quad \ldots \quad 1]^{T} \tag{69}$$

an have similar expressions for the quantities A^{fg}_{eh}, D^{ah}_{dc}, D^{fg}_{eh}, F^{++}, F^{+-}, F^{--}, Φ^{+}, Φ^{-} can write equations (60) and (61) in the form of the interaction principle given by aiah 1984)

$$\begin{bmatrix} U^{+}_{l} \\ U^{-}_{l-1} \end{bmatrix} = \begin{bmatrix} t(l,l-1) & r(l-1,l) \\ r(l,l-1) & t(l-1,l) \end{bmatrix} \begin{bmatrix} U^{+}_{l-1} \\ U^{-}_{l} \end{bmatrix} + \begin{bmatrix} \Sigma^{+} \\ \Sigma^{-} \end{bmatrix} \tag{70}$$

re t(l,l-1), t(l-1,l), r(l,l-1), r(l-1,l) are the transmission and reflection matrices, and and Σ^{-} and the internal source terms

e write,

$$X_1 = A^{fg}_{eh} - \sigma\tau^{+}F^{++}_{l},\ X_2 = \sigma\tau^{-}F^{+-}_{l-1}$$

$$X_3 = \sigma\tau^{+}F^{-+}_{l},\quad X_4 = D^{ab}_{dc} - \tau^{-}\sigma F^{--}_{l-1}$$

$$Y_1 = A^{ab}_{dc} - \sigma\tau^{-}F^{++}_{l-1},\ Y_2 = \sigma\tau^{+}F^{+-}_{l}$$

$$Y_3 = \sigma\tau^{-}F^{-+}_{l-1},\ Y_4 = D^{fg}_{eh} - \sigma\tau^{+}F^{--}_{l} \tag{71}$$

, the transmission and reflection operators are written as,

$$t(1,1-1) = R^{+-} X_1^{-1}[X_2 X_4^{-1} Y_3 - Y_1] \tag{72}$$

$$t(1-1,1) = R^{-+} X_4^{-1}[X_3 X_1^{-1} Y_2 - Y_4] \tag{73}$$

$$r(1,1-1) = R^{-+} X_4^{-1}[Y_3 - X_3 X_1^{-1} Y_1] \tag{74}$$

$$r(1-1,1) = R^{+-} X_1^{-1}[Y_2 - X_2 X_4^{-1} Y_4] \tag{75}$$

$$R^{+-} = [I - X_1^{-1} X_2 X_4^{-1} X_3]^{-1} \tag{76}$$

$$R^{-+} = [I - X_4^{-1} X_3 X_1^{-1} X_2]^{-1} \tag{77}$$

$$\Sigma^{+}_{1-\frac{1}{2}} = \sigma R^{+-} X_1^{-1}[(\tau^{-}\Phi^{+}_{1-1} B^{+}_{1-1} + \tau^{+}\Phi^{+}_{1} B^{+}_{1}) + X_2 X_4^{-1}(\tau^{-}\Phi^{-}_{1-1} B^{-}_{1-1} + \tau^{+}\Phi^{-}_{1} B^{-}_{1})] \tag{78}$$

$$\Sigma^{-}_{1-\frac{1}{2}} = \sigma R^{-+} X_4^{-1}[\tau^{-}\Phi^{-}_{1-1} B^{-}_{1-1} + \tau^{+}\Phi^{-}_{1} B^{-}_{1}) + X_3 X_1^{-1}(\tau^{-}\Phi^{+}_{1-1} B^{+}_{1-1} + \tau^{+}\Phi^{-}_{1} B^{-}_{1})] \tag{79}$$

The method described above is employed to calculate line profiles emerging out of spherically symmetric and expanding atmospheres The atmosphere is divided into several shells (spherically symmetric) and the reflection and transmission matrices are calculated These operators are used to estimate diffuse radiation field throughout the medium in which the lines are formed. We use the algorithm described in Peraiah (1984) We present the results of the calculation of lines, by this method, in the next section

III. Discussion of the Results

The medium is divided into n spherically symmetric shells where $n = 1$ at $\tau = 0$ and $n = n_{max}$ at $\tau = \tau_{max}$ We have chosen B/A = 1,5,2, and 3 where B and A are the outer and inner radii of the spherical medium respectively The density and radial velocity are assumed to vary in accordance with the equation of continuity which is given by

$$4\Pi r^2 \rho V = \text{constant} \tag{80}$$

Where ρ is the density and V is the radial velocity at the radial point r These calculations are meant to bring out the effects of density and velocity gradients on the formation of spectral lines in spherical media by employing the method described in the previous section Therefore we have chosen parametrised quantities of ϵ, β, B/A, B(r) the Planck

tion and velocities of radial expansion. The velocities are expressed in terms of the n thermal units (mtu).

considered two cases:

$$(1) \quad \rho(r) \sim r^{-2}, \; V(r) = \text{constant} \tag{81}$$

$$(2) \quad \rho(r) \sim r^{-3}, \; V(r) \sim r \tag{82}$$

the purpose of calculating the optical depth we assumed an electron density at A inner radius) so that we can calculate the optical depth in a realistic way. We set

$$Ne \; (A) = 10^{14} \text{ or } 10^{15} \text{ cm}^{-3} \tag{83}$$

re A is taken to be equal to 10^{12} cm.

divide the medium into a number of spherically symmetric shells and calculate the ection, transmission operators and the source vectors given in equations (72) to (79) ach shell. By using this information the diffuse radiation field is calculated by employ- the formulation given in Peraiah (1974). We have employed 9 trapezoidal points on frequency grid and 2 points of Gauss-Legendre polynomial on the angle grid of half e. These are found to give enough accuracy which is confirmed through the principle flux conservation (see Paper I). The number of shells change from case to case as depends on the total optical depth T and the geometrical extension B/A. With increasing nd B/A, the total number of shells also increases. From an analysis of the X_1^{-1} and matrics (see equations 72 to 75) found in transmission and reflection operators the $_t$ (see Paper I) is found to be about 0.5. However this changes considerably when we oduce the velocity gradients.

In order to avoid the amount of calculations we employ a small number of shells y about 30) and engage the star algorithm (Peraiah 1984). If τ_{crit} is less than 0.1 then used the doubling algorithm by making $(\Delta r/\bar{r})_{subshell}$ constant over all the subshells. e division of a shell into subshells is necessitated because of τ_{crit}). This is one way of eding up the calculations with some loss of accuracy.

e boundary conditions we employ are given as follows:

$$U_1^+ (\tau = 0, \mu_j) = 0$$

$$U^{-}_{N+1}(\tau = T, \mu_j) = 1 \quad \text{for } \epsilon = \beta = 0 \tag{84}$$

$$B(r) = 0$$

And

$$U^{+}_{1}(\tau = 0, \mu_j) = 0$$

$$U^{-}_{N+1}(\tau = T, \mu_j) = 0 \text{ for } \epsilon = \beta > 0 \tag{85}$$

$$B(r) = 1$$

The boundary conditions of velocity are set in accordance with equations (81) and (82) and velocities are expressed in mean thermal units (mtu) When we consider equation (81), we set $V(\tau = T) = V(\tau = 0) = V_{max}$ and in the case of equation (82), we set $V(\tau = T) = 0$ and $V(\tau = 0) = V_{max}$. The velocities shown in the figures correspond to V_{max} When the solution of the problem is obtained, we calculate the source function given in equation (26). The source function thus obtained is in the comoving frame By using this source function we can transform the radiation field on to an observer's frame at infinity as shown in Figure 2. The procedure is described in Peraiah (1984)

In figures (3) to (8) we have plotted the variation of source functions along the optical depth, for the parameters shown in each figure. These are some of the typically varying source functions. We need not show all the other results as we do not find changes very much different from what are presented in Figures (3) to (8). The source function changes smoothly from its maximum value at $\tau = T$ to its minimum value at $\tau = 0$. When the motion is introduced its value diminishes at every point on the τ coordinate.

The number of free parameters in this problem is very high and therefore we are forced to choose few representative cases that imitate the stellar atmospheric conditions. In Figures (9) to (31), the flux profiles of the lines are given against the standardised frequency points Q where

$$\pm Q = \pm \frac{(X + V)}{|X_{max}| + V_{max}} \tag{86}$$

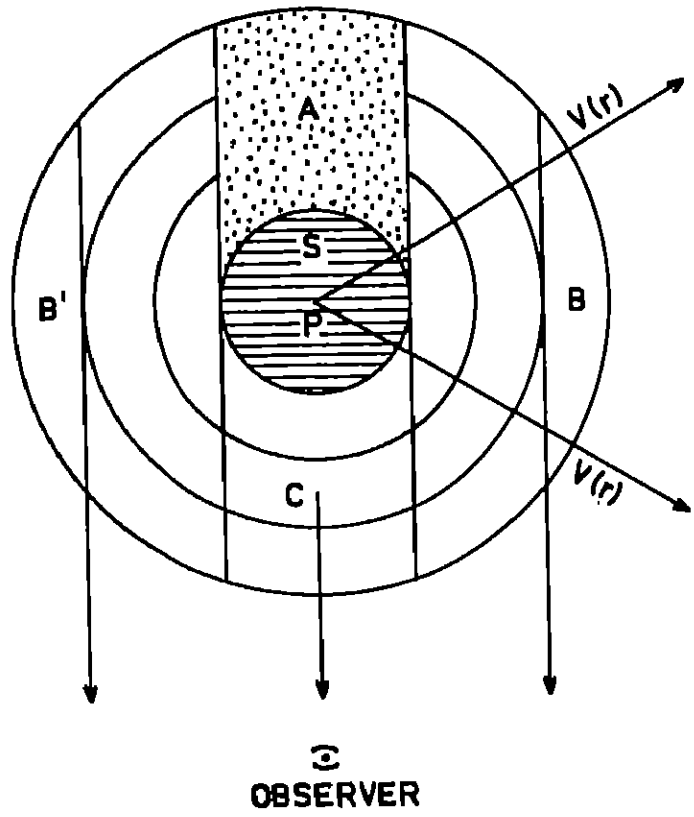

Fig. 2 Schematic diagram of expanding envelope. P is the centre of the star S. The region A is occulted from the view of the observer. The matter is flowing radially outwards as shown with velocity V(r). The radiation from lobes B and B' gives emission profiles. The radiation from the region C which is directly in between the star and the observer gives rise to the absorption component.

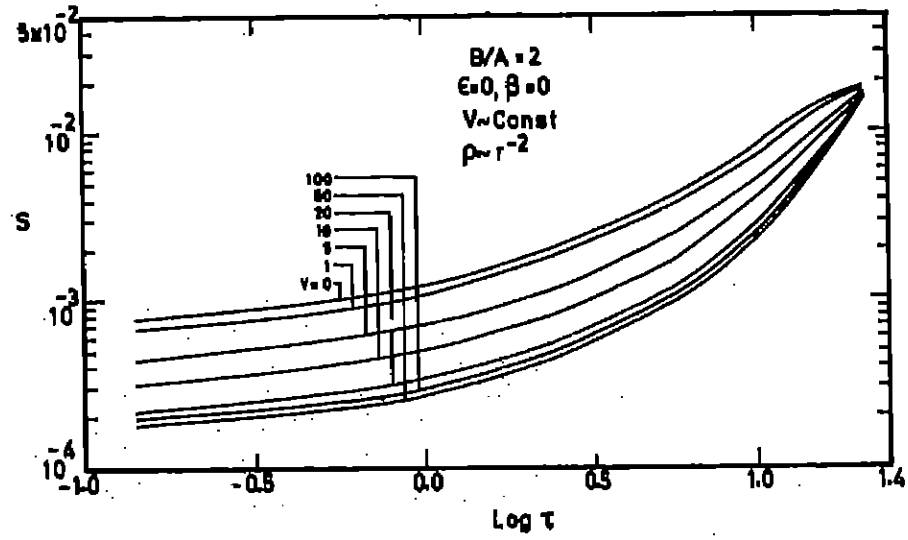

Fig.3 Source function versus optical depth for the velocity and other physical parameters as shown in the figure.

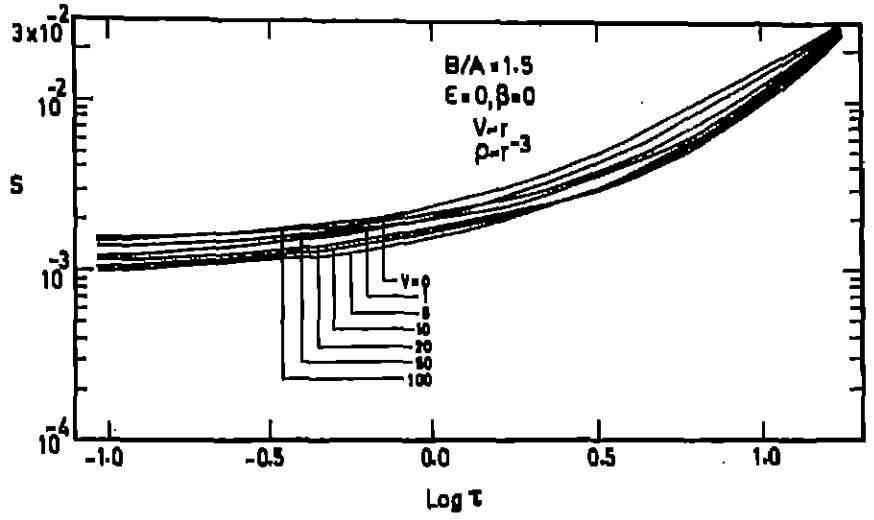

Fig.4 Source function versus optical depth.

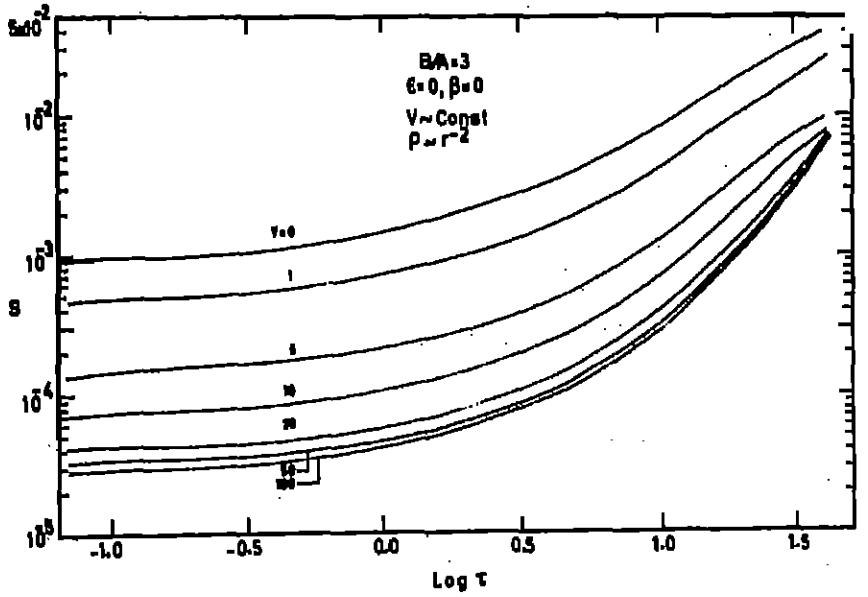

Fig.5 Source function versus optical depth.

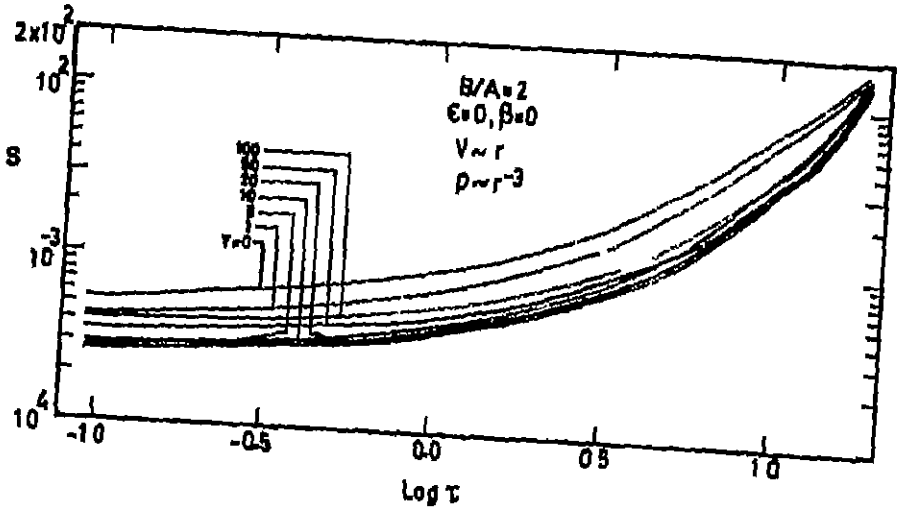

Fig 6 Source function versus optical depth

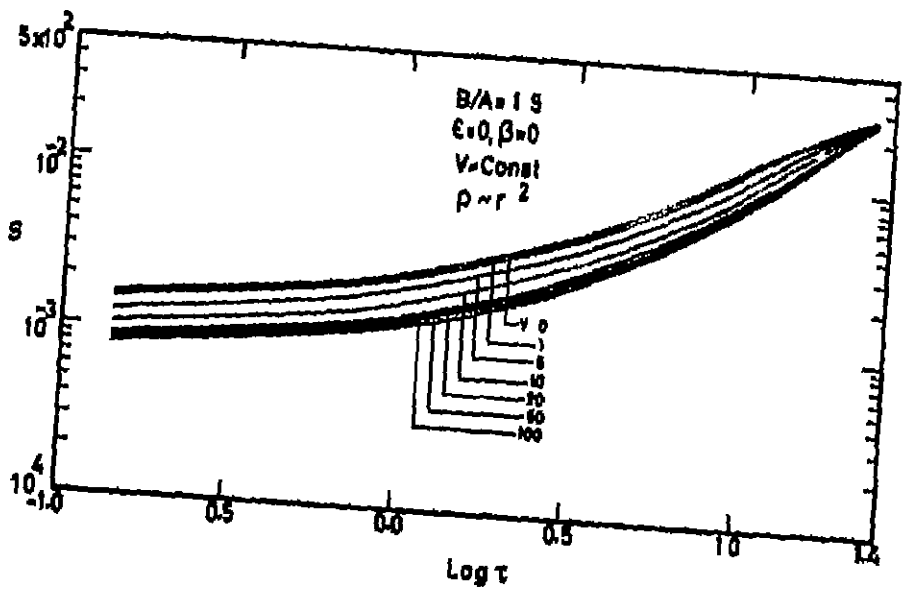

Fig 7 Source function versus optical depth

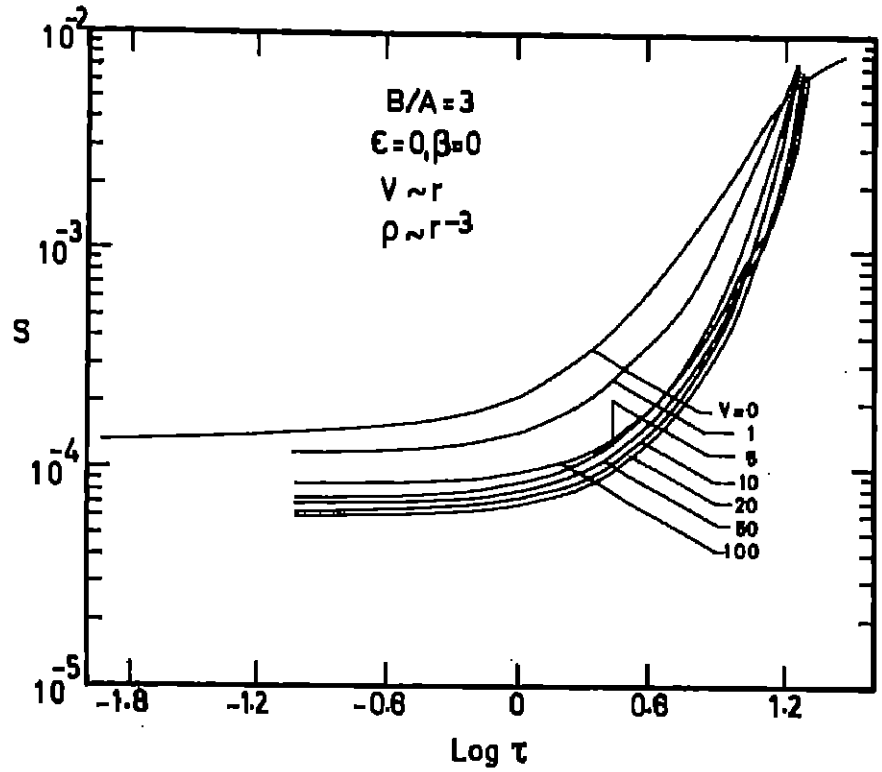

Fig.8 Source function versus optical depth.

This type of formulation along the abscissal permits us to plot the profiles for different velocities in the same figure without loosing any information such as shape of the line, shifts of the line centres etc. Figure 9 contains the profiles for B/A = 1.5, $\epsilon = 0$, $\beta = 0$ and T = 21. We have employed constant velocities of V = 0,1,5,10,20,50 and 100 mtu. When V = 0, we obtain a symmetric profile with a small amount of emission in the wings on both sides of the centre of line. This is primarily due to sphericity effects. When velocity V = 1 mtu is introduced, we obtain, a line whose emission on the redside increases considerably while the blue emission disappears. Further more the absorption part of the line shifts to blue side by almost one mean thermal unit. When V is increased to 5 mtu the red emission increases further and the blue absorption shifts by a considerable amount and a P Cygni type of profile is generated. As we increase the velocity both red emission and blue absorption reduce. When V = 50 or 100 the emission part becomes flatter and the absorption is reduced and the shift in the absorption is not exactly equal to the expanding velocity. The line profiles change considerably depending on the velocity gradients. We employed a constant velocity in this case and therefore the velocity gradients $\frac{dV(r)}{dr}$ do

exist. However if we see equation (24) and (25), we find that the factor $(1 - \mu^2)\ \frac{V(r)}{r}$ ts in the frequency derivative term. Although V remains constant, as r increases towards surface, $\frac{V(r)}{r}$ acts like a velocity gradient. Therefore, the profiles we presented in figure really show the effects of velocity gradients.

We have measured the shifts of the centre of the line from the rest position and ratios h_e/h_a and A_e/A_a where h_e and h_a are the emission and absorption heights and ires 9a, 10a etc., corresponding to the profiles given in Figures 9 and 10 etc., respecly. The quantities h_e/h_a, A_e/A_a and shifts in mtu can be easily measured in an observed . We can therefore immediately compare these with the models presented in this paper obtain approximate data regarding velocities of expansion, densities, and other aspects.

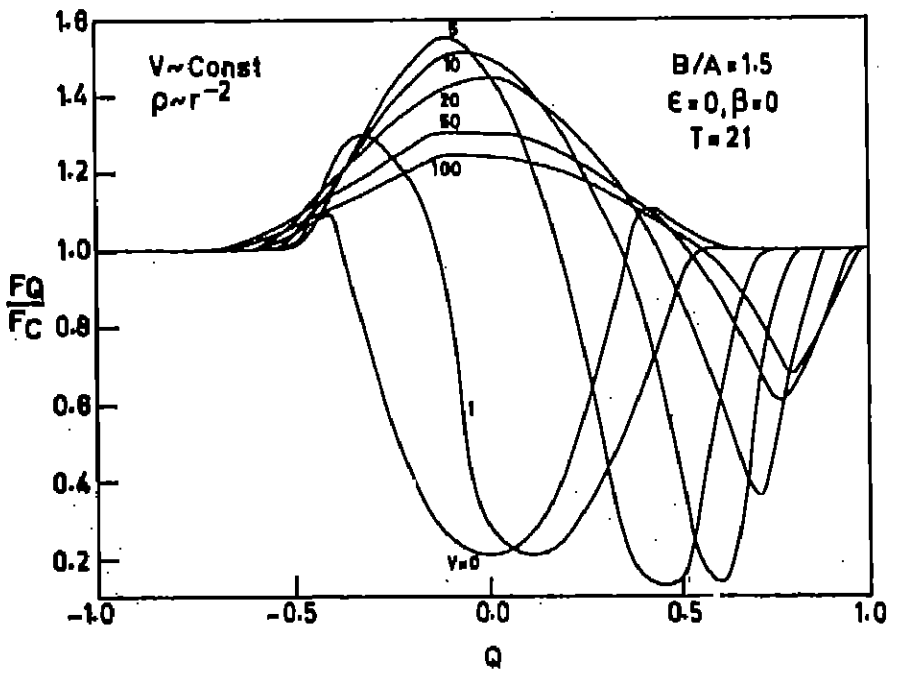

Fig. 9. Line profiles given for flux versus standardised frequency Q.

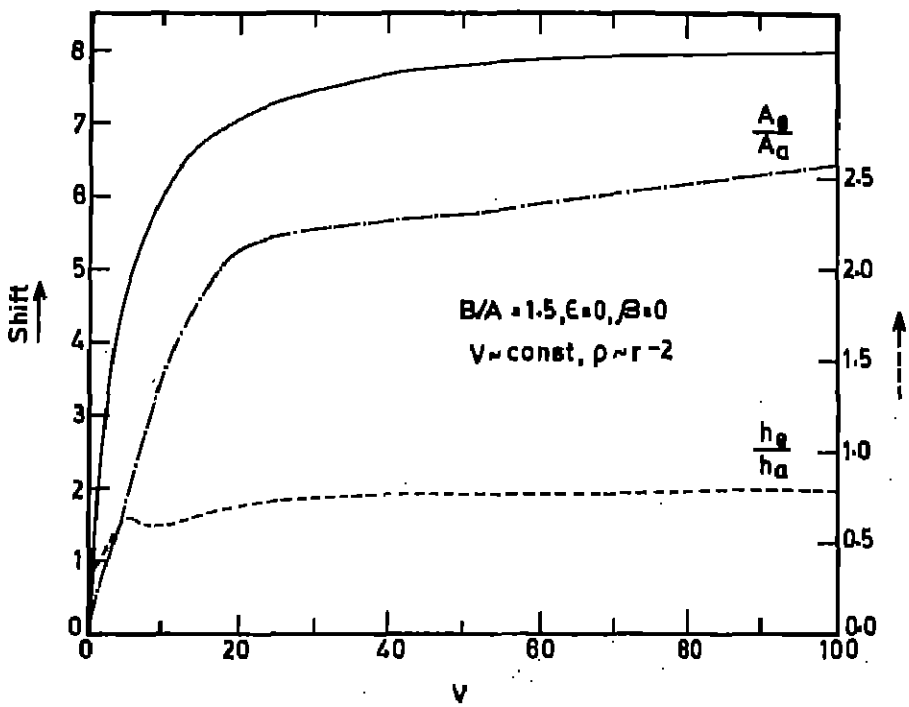

Fig. 9a The values of h_e/h_a and A_e/A_a and the shift of the centre of the line in mean thermal units are given. The scale on the ordinate on the right hand side represent the above two ratios and the shift is shown on the ordinate on the left hand side. These ratios and shifts correspond to the profile shown in figure 9a.

In Figure 10, we employed the same values for the parameters ε, β, B/A as in Figure 9, but with $\rho \sim r^{-3}$ and $V \sim r$. The optical depth used in this case is smaller than that used in Figure 9, because the density is changing as r^{-3} instead of r^{-2}. When there is no motion, the profile is symmetric and this becomes increasingly asymmetric as the velocity increases. The absorption component becomes flat bottomed for larger velocities. Figure 11 shows flux profiles for $\varepsilon = 10^{-3}$ and $\beta = 0$ with $\rho \sim r^{-2}$ and V = constant. We introduce Planck function such that,

$$4\pi r^2 B(r) = 1. \tag{87}$$

where B(r) is the Planck function.

In a static medium we obtain an emission line with absorption at the line centre.

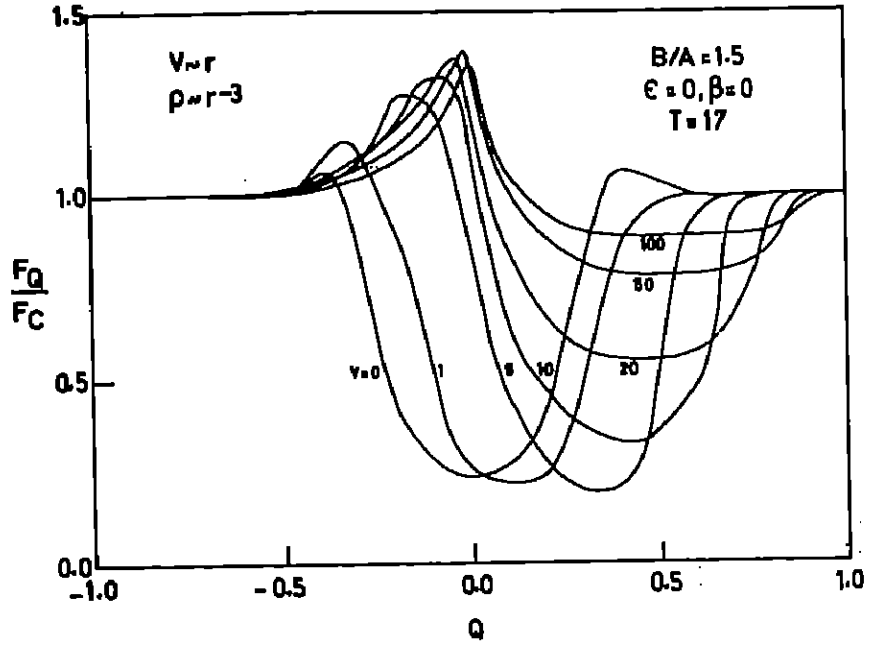

Fig.10 Line profiles given for flux versus standardised frequency Q

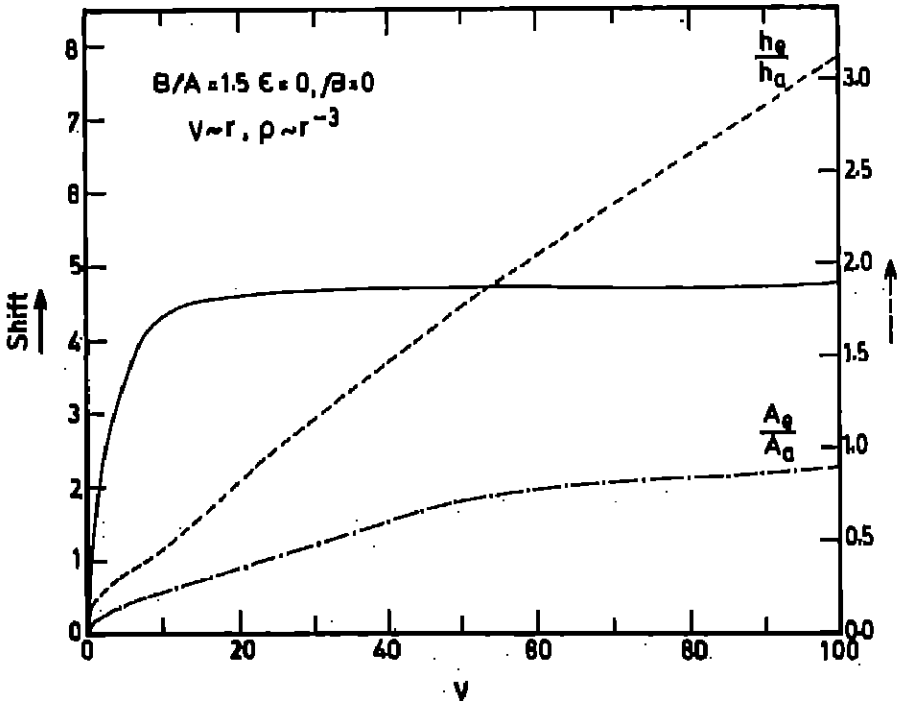

Fig.10a. h_e/h_c and A_e/A_c and the shifts correspond to the profile shown in figure 10

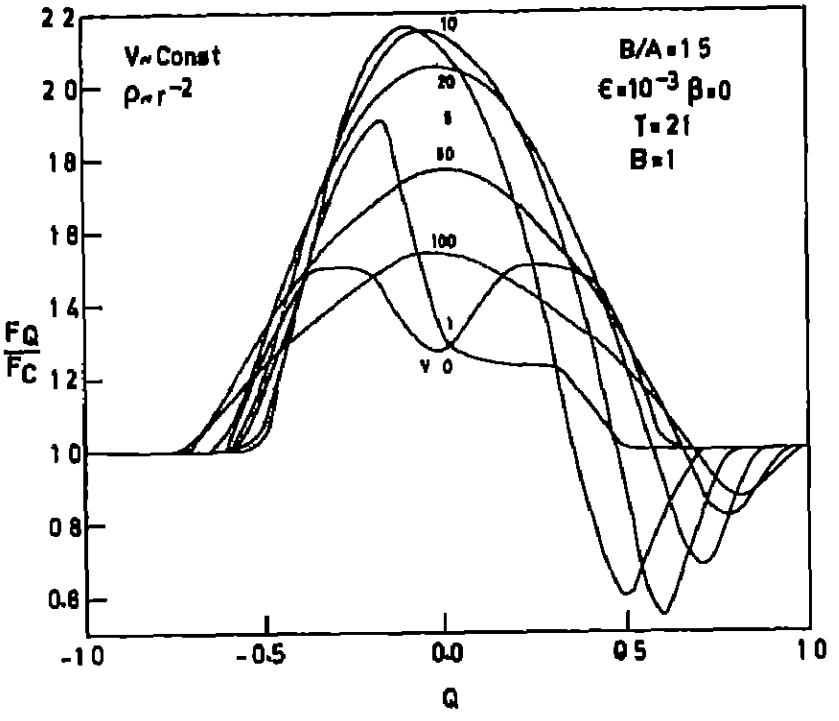

Fig 11 Line profiles with $4\pi r^2 B(r) = 1$

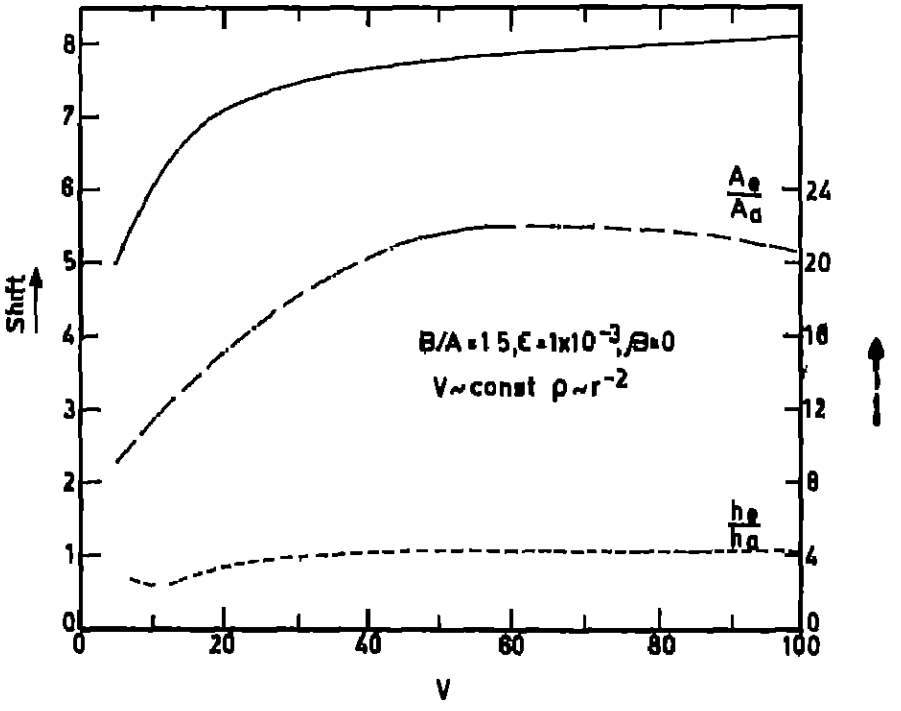

Fig 11a h_e/h_a and A_e/A_a and the shifts correspond to the profile shown in Figure 11

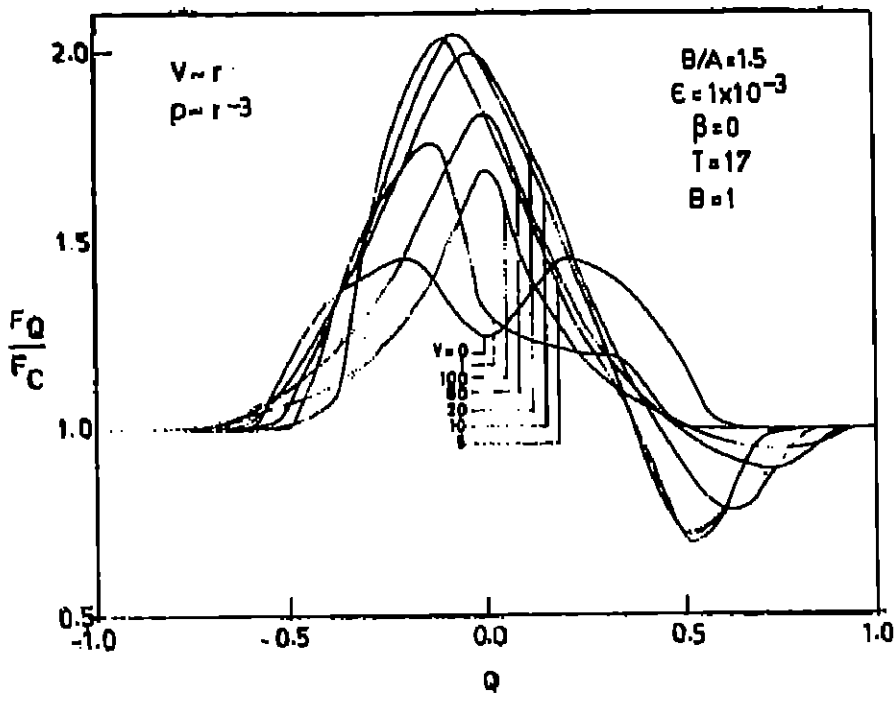

Fig.12 Line profiles with $4\pi r^2$ B(r) =1

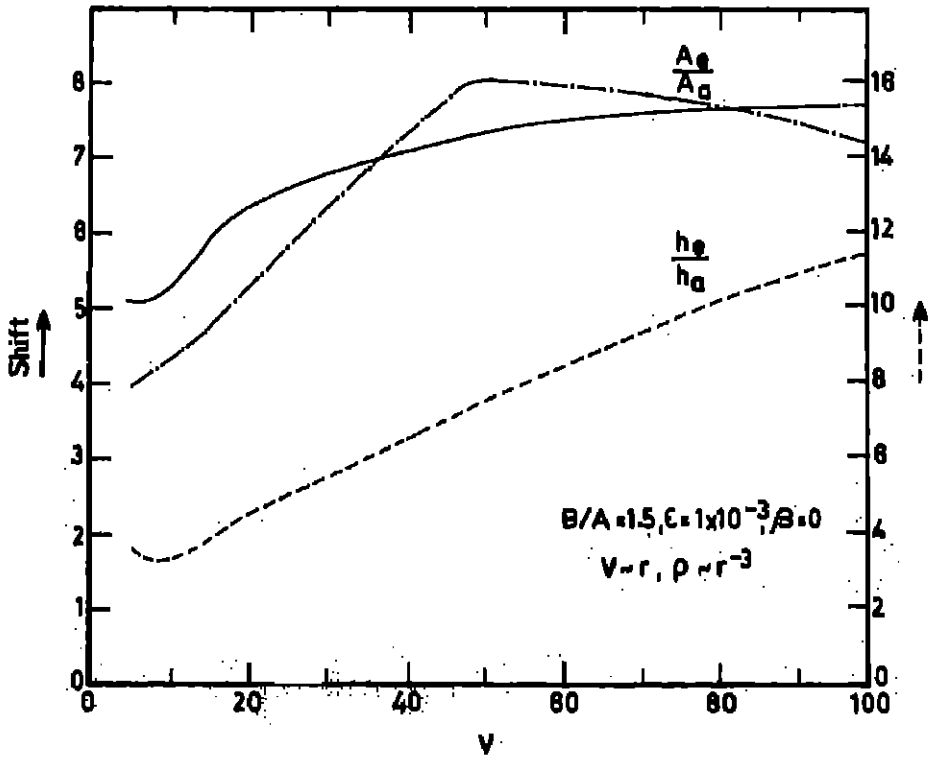

Fig.12a h_e/h_a and A_e/A_a and the shifts correspond to the profile shown in Figure 12

When $v > 0$, the emission on red side increases whereas emission on the blue side gradually reduces and becomes deep absorption with its characteristic shift from the centre of the line. We should note one important aspect here, that is, the emission peaks for any velocity do not shift from the centre of the line whereas the absorption shifts proportionately with the velocity of expansion. Flux profiles for $\rho \sim r^{-3}$ and $V \sim r$, $\epsilon = 10^{-3}$, $\beta = 0$ and $4\pi r^2 B(r) = 1$ are given in Figure 12. These profiles exhibit the same features as those given in Figure 11. In Figure 13, we present flux profiles with emission from the continuum with a small continuum optical depth equal to 21×10^{-3} and $\rho \sim r^{-2}$ and V = constant. The profile of the static medium is an absorption line with considerable amount of emission near the wings. Introduction of radial velocities increase the emission on the red side while reducing it on the blue side. For higher velocities of expansion, the emission is reduced without getting shifted from the centre of the line, while the blue shift of absorption part remains proportional to the expansion velocity. In Figure 14, we have plotted flux profiles for $\rho \sim r^{-3}$ and $V \sim r$. These profiles show characteristics similar to those given in Figure 13.

We have increased the geometrical extension to $B/A = 2$ and repeated the calculations and presented these results in Figures (15) to (20). A comparison of these figures with those given in Figures (9) to (14) reveals the fact that the physical characteristics are same in both cases except for the fact that the lines in the former case are broader than in the latter. Profiles presented in Figures (21) to (25) are calculated with $B/A = 3$. Again these profiles are similar in their physical characteristics to those presented earlier. So far, we employed optical depths which are not very large. In Figure 26 we plotted profiles for $B/A = 3$, $\epsilon = \beta = 0$ and $T = 450$ which is nearly 10 times as large as that used in Figure 21. These profiles are completely absorption lines. They become narrow as the expansion velocities are increased. The shift of the line centre is again proportional to the expansion velocity. Figure 27 gives the profiles for $\rho \sim r^{-3}$ and $v \sim r$. These profiles become deeper as the velocities of expansion increase. In Figures (28) and (29) we have given the profiles $T = 300$ and 450 respectively. These profiles are computed with $\epsilon = 10^{-3}$ and $4\pi r^2 B(r) = 1$. They behave as those presented in Figures (9) to (25) with line or continuum emission. In Figures (30) and (31), we have calculated the ratios of he/ha, Ae/Aa and the line shifts corresponding to the values of the parameters shown in the respective figures without showing the corresponding line profiles.

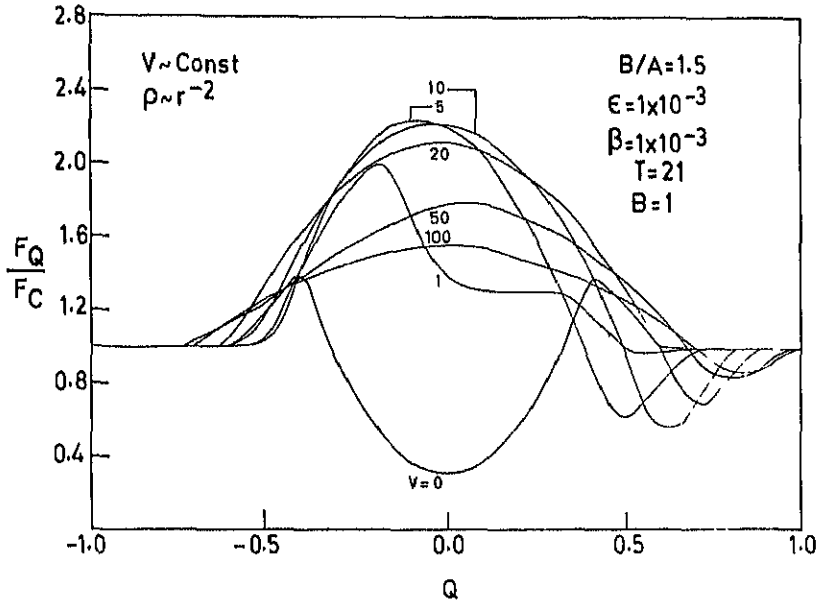

Fig.13 Line profiles with $4\pi r^2 B(r) = 1$

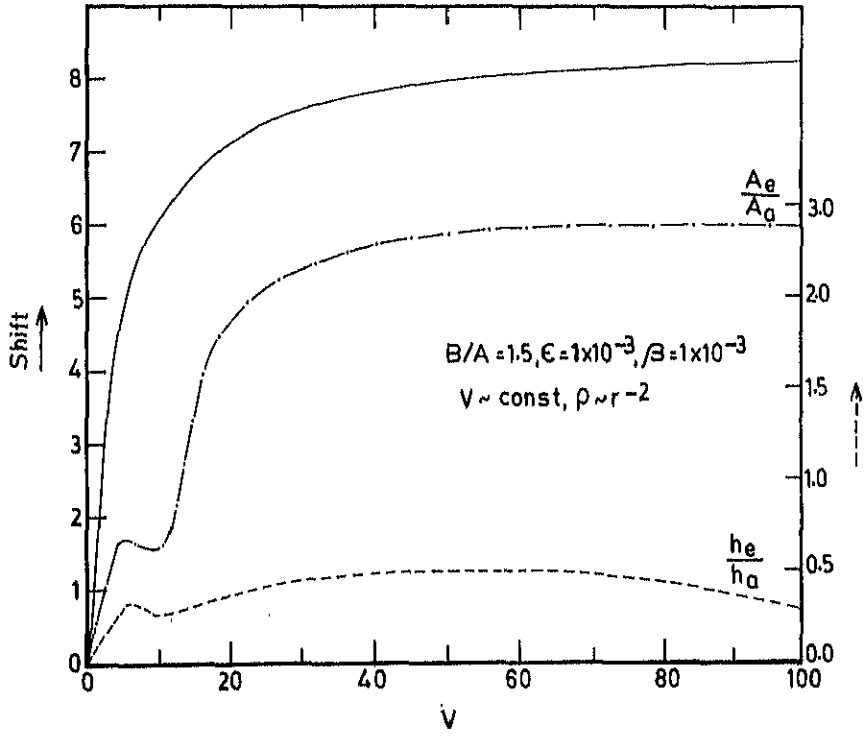

Fig.13a h_e/h_a and A_e/A_a and the shifts correspond to the profile shown in Figure 13

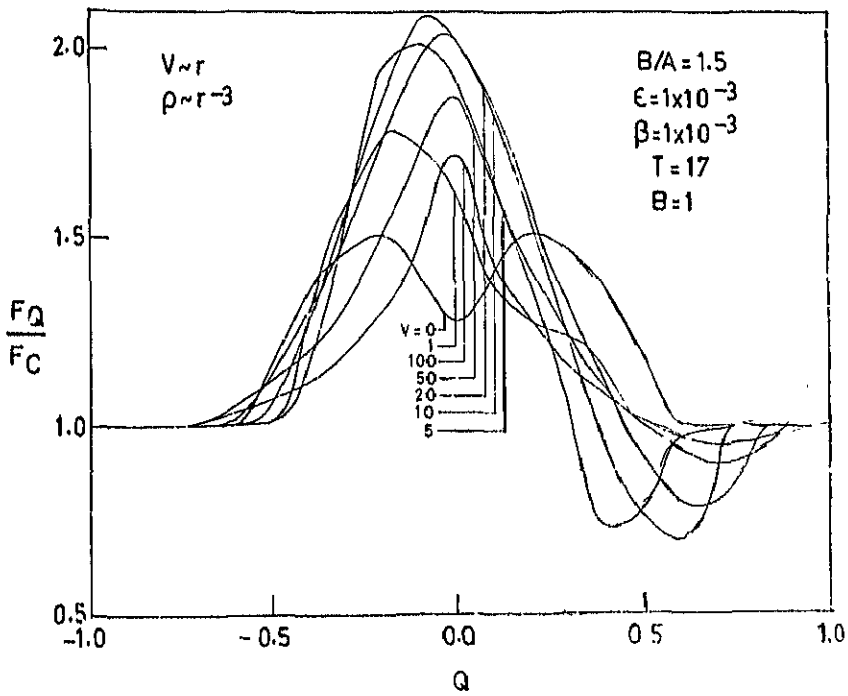

Fig.14 Line profiles with $4\pi r^2 B(r) = 1$

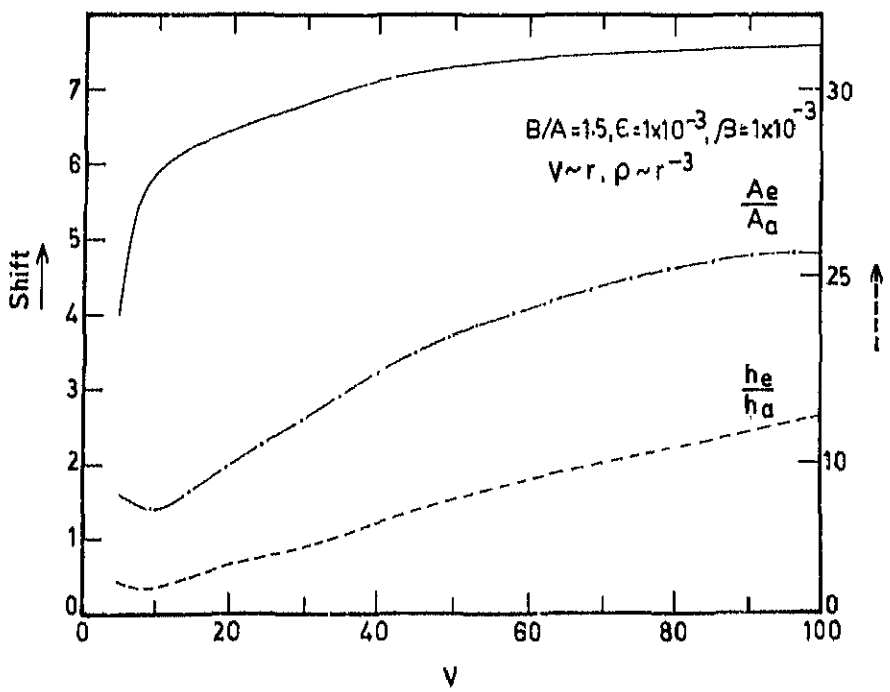

Fig.14a h_e/h_a and A_e/A_a and the shifts correspond to the profile shown in Figure 14

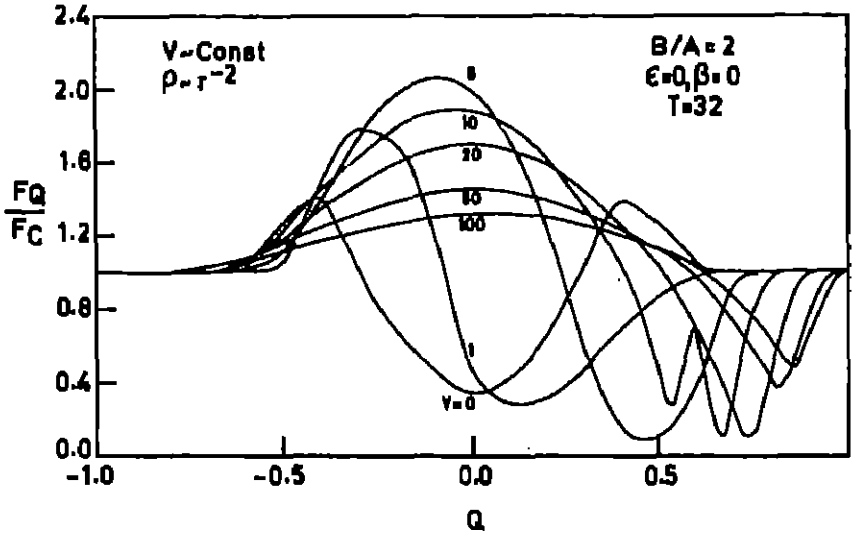

Fig.15 Line profiles

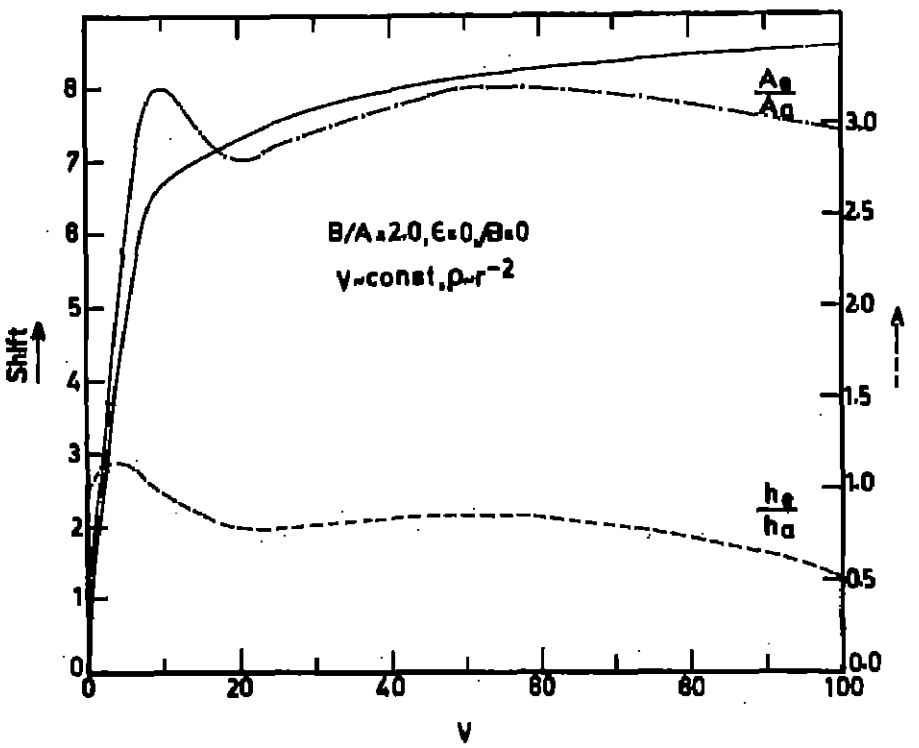

Fig.15a h_e/h_a and A_e/A_a and the shifts correspond to the profile shown in Figure 15

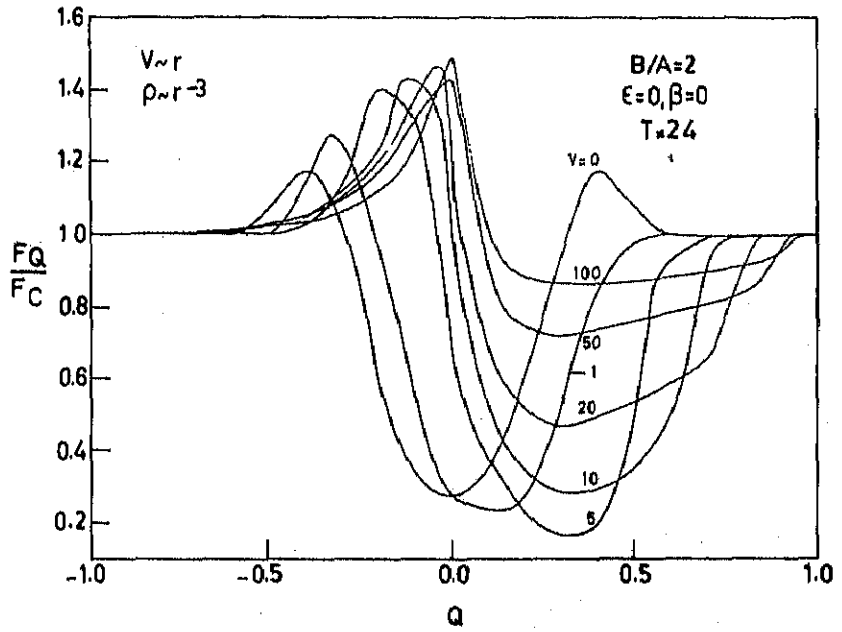

Fig.16 Line profiles.

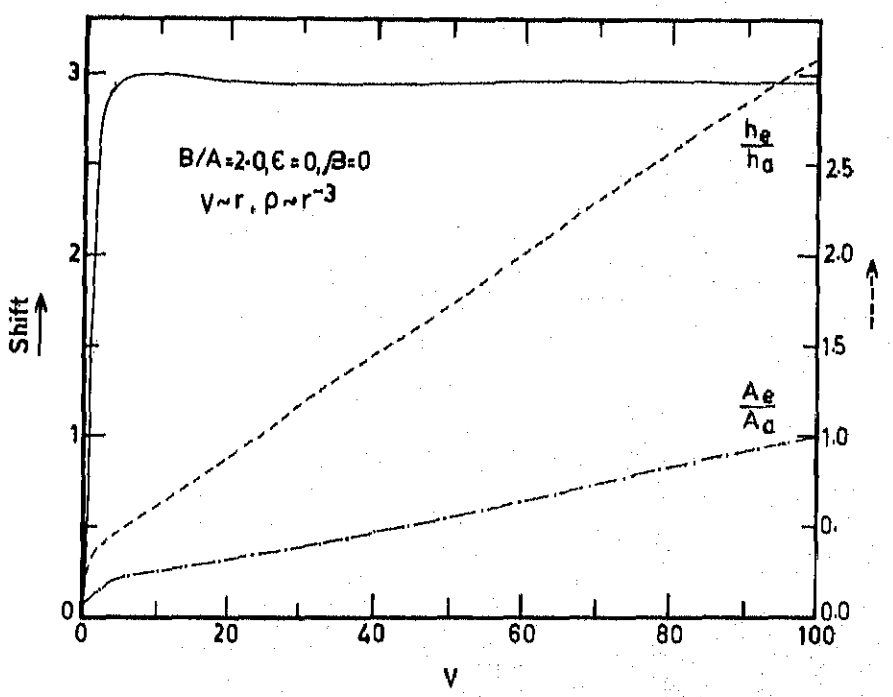

Fig.16a h_e/h_a and A_e/A_a and the shifts correspond to the profile shown in Figure 16

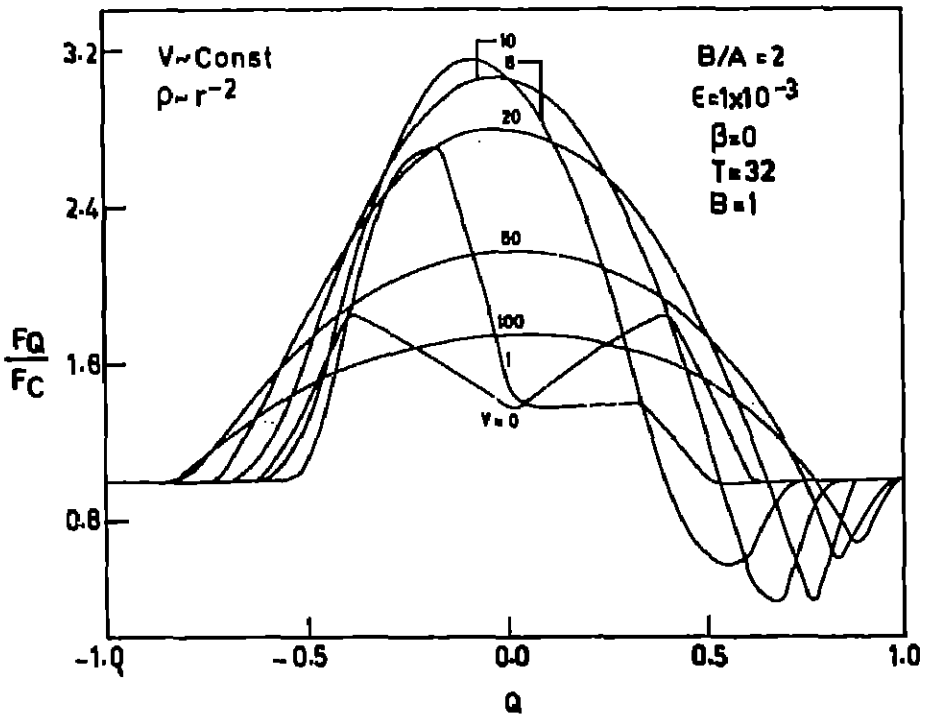

Fig.17 Line profiles with $4\pi r^2 B(r) = 1$

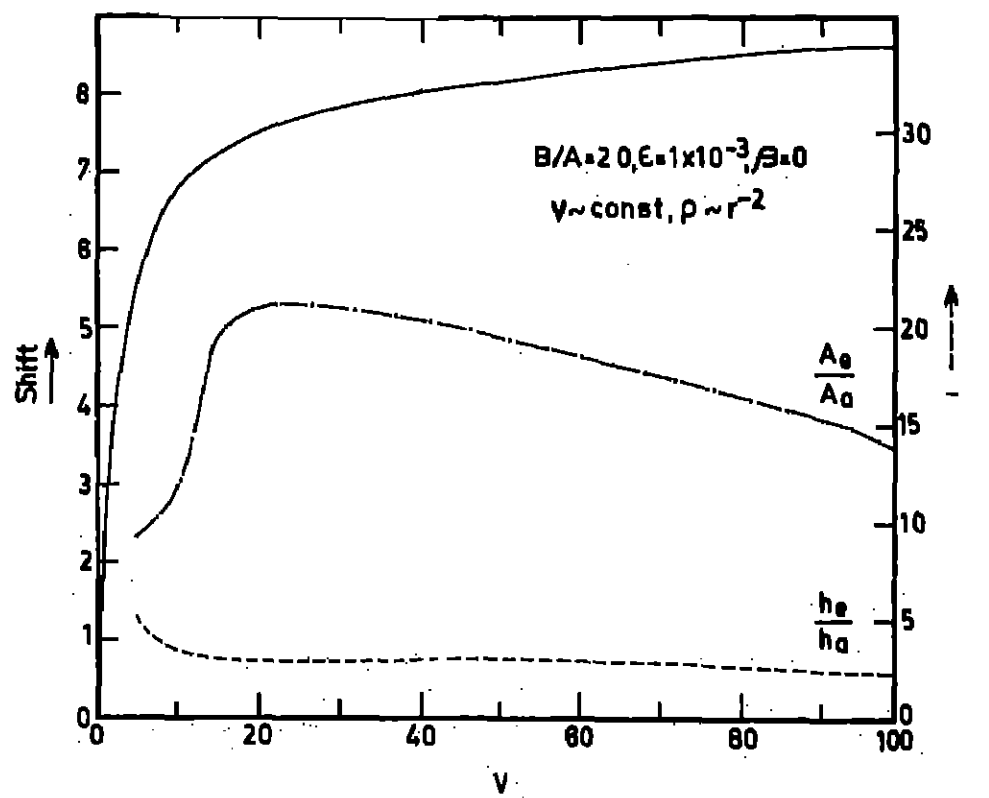

Fig.17a h_e/h_a and A_e/A_a and the shifts correspond to the profile shown in Figure 17

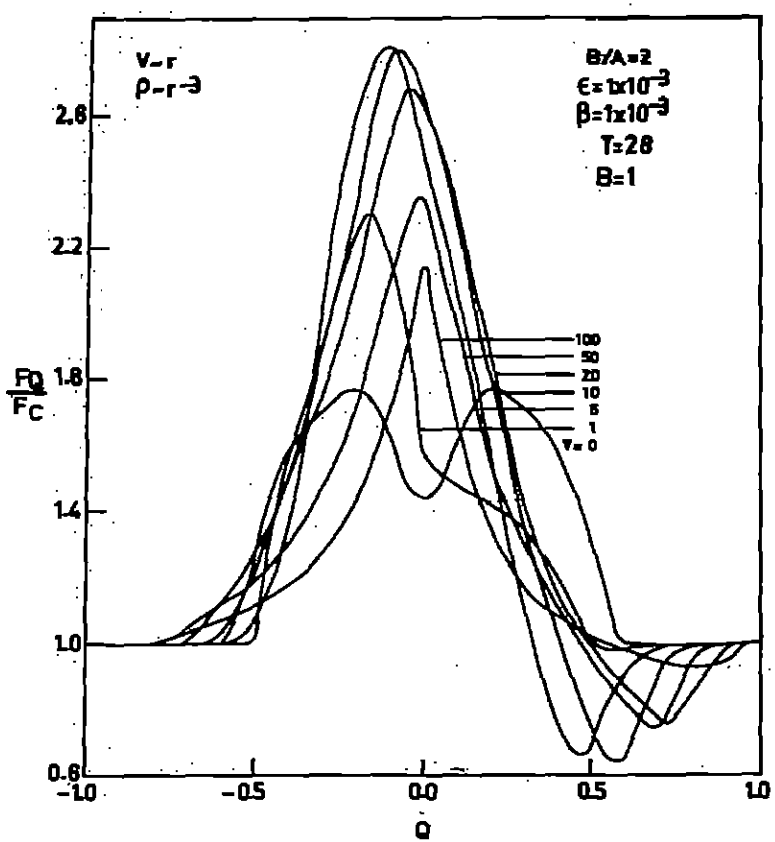

Fig.18 Line profiles with $4\pi r^2 B(r) = 1$

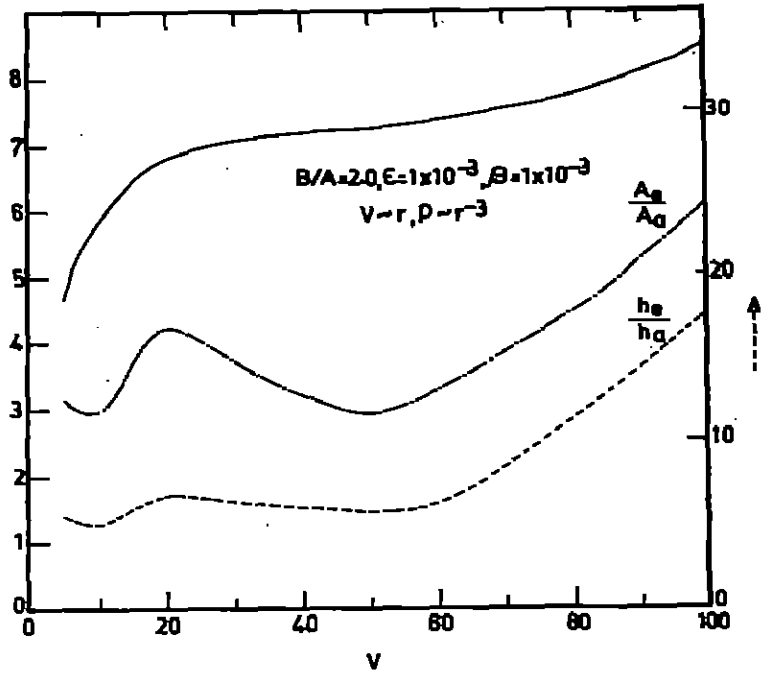

Fig.18a h_e/h_a and A_e/A_a and the shifts correspond to the profile shown in Figute 18

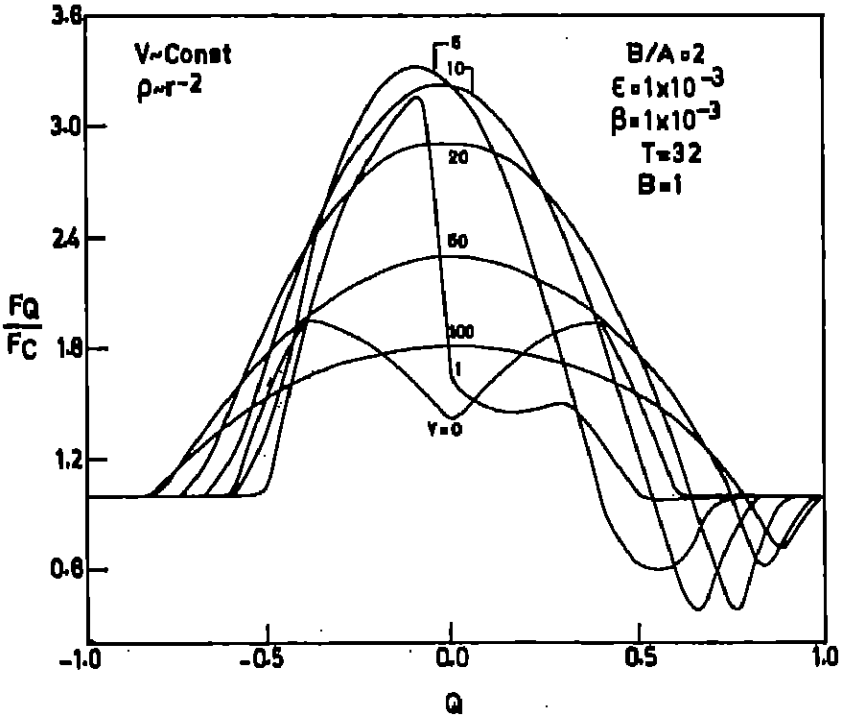

Fig.19 Line profiles with $4\pi r^2 B(r) = 1$

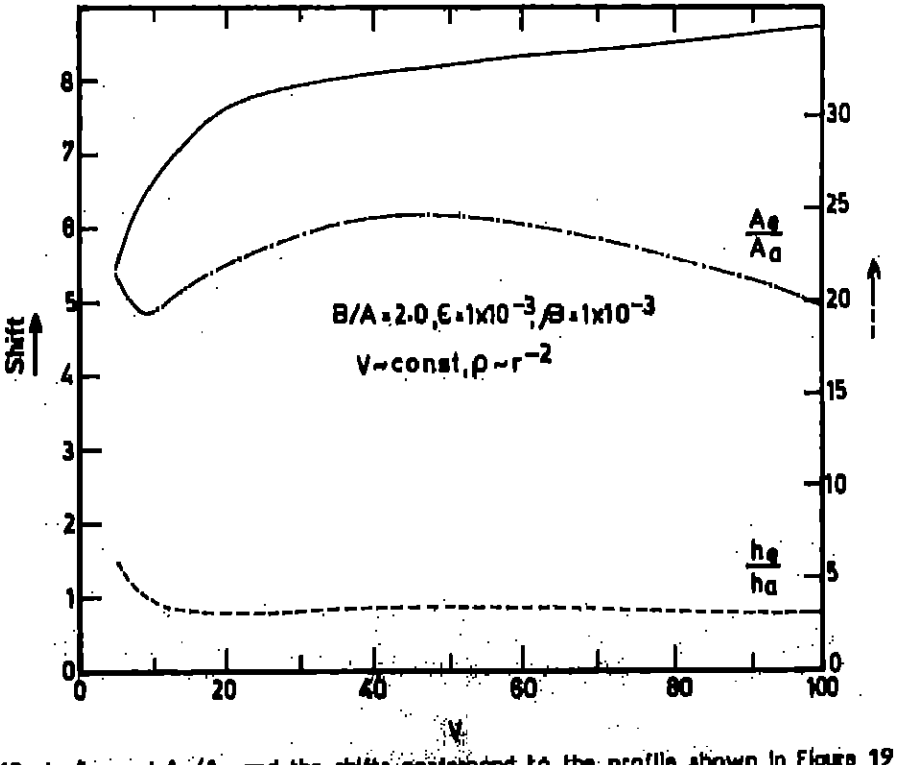

Fig.19a h_e/h_a and A_e/A_a and the shifts correspond to the profile shown in Figure 19

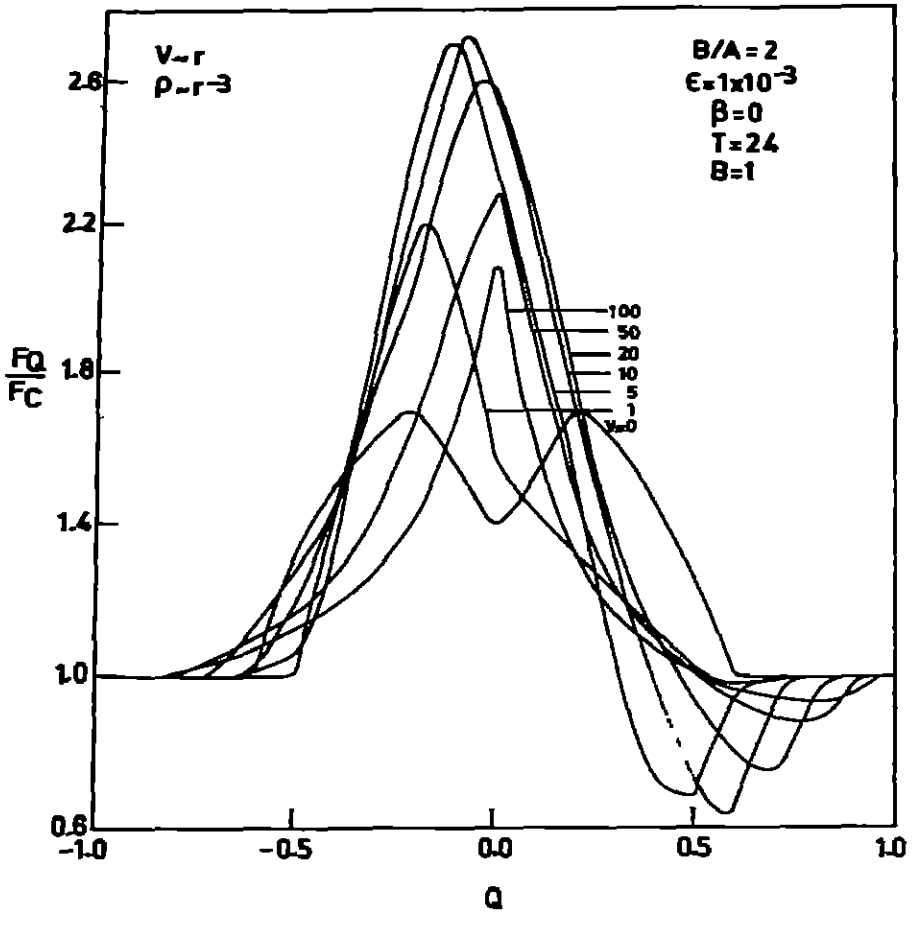

Fig.20 Line profiles with $4\pi r^2 B(r) = 1$

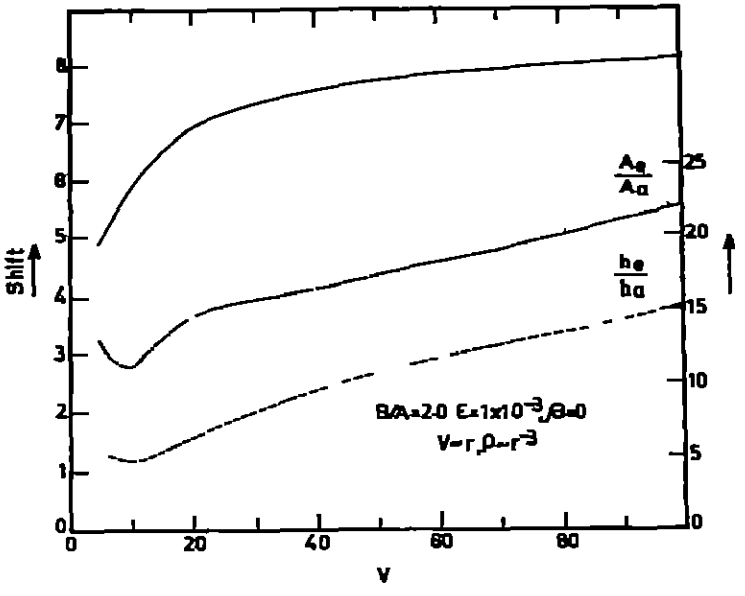

Fig 20a h_e/h_a and A_e/A_a and the shifts correspond to the profile shown in Figure 20

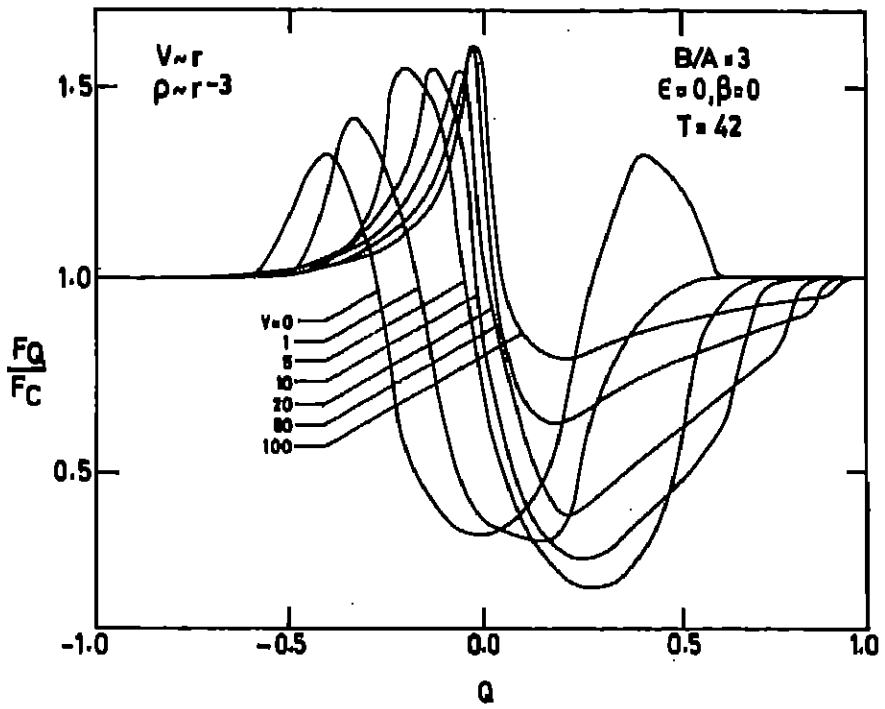

Fig.21 Line profiles.

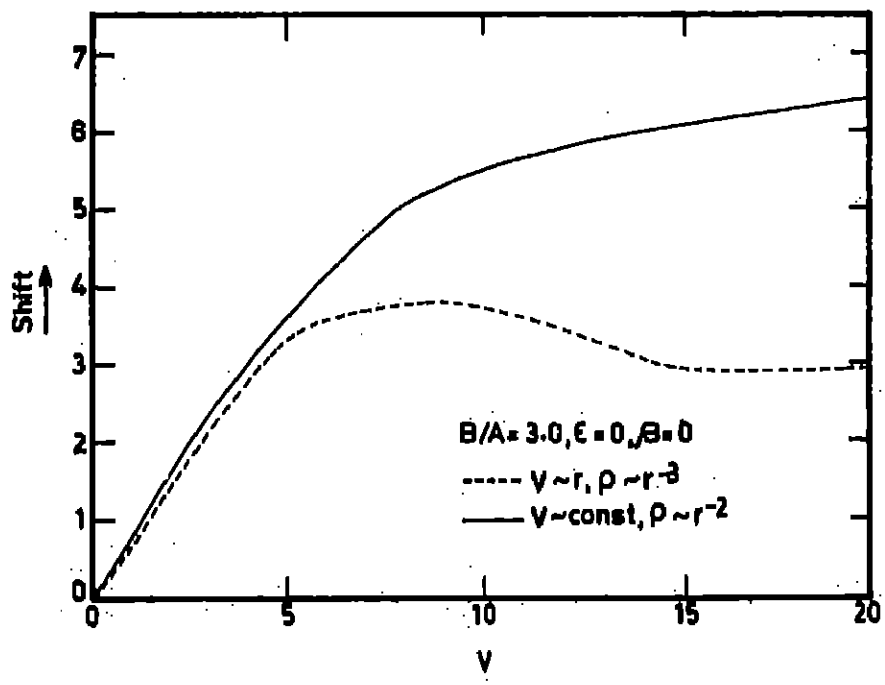

Fig.21a h_e/h_a and A_e/A_a and the shifts correspond to the profile shown in Figure 21

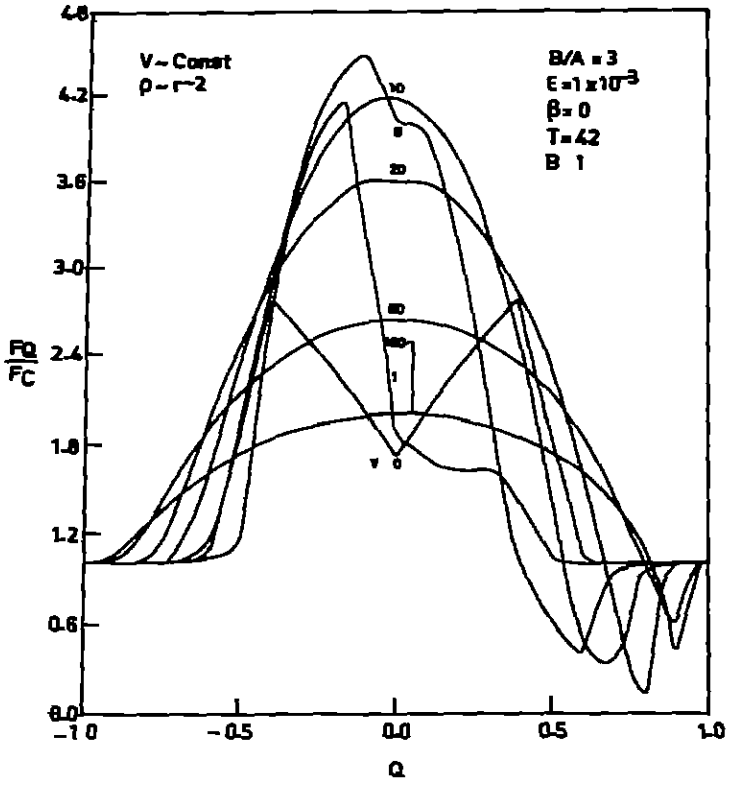

Fig.22 Line profiles with $4\pi r^2$ B(r) = 1

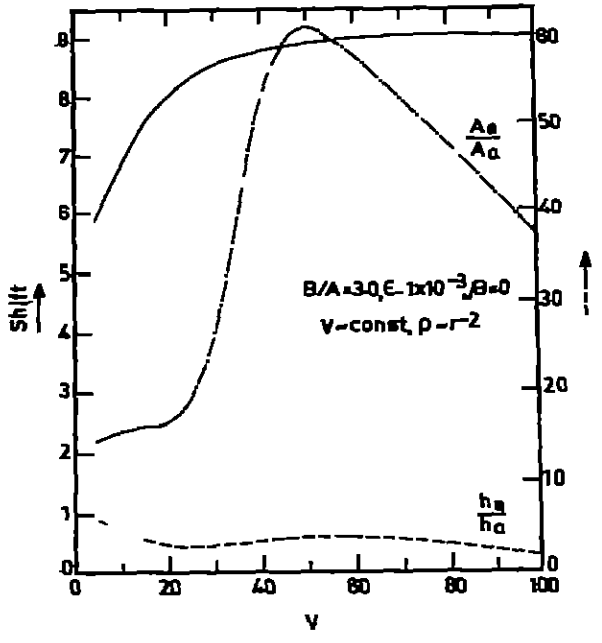

Fig.22a h_e/h_a and A_e/A_a and the shifts correspond to the profile shown in Figure 22

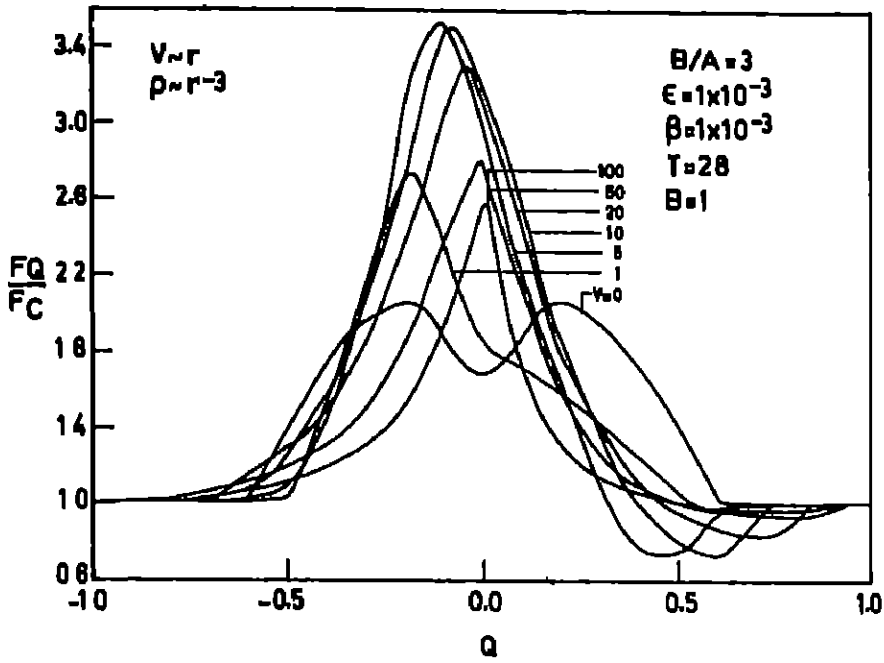

Fig 23 Line profiles with $4\pi r^2 B(r) = 1$

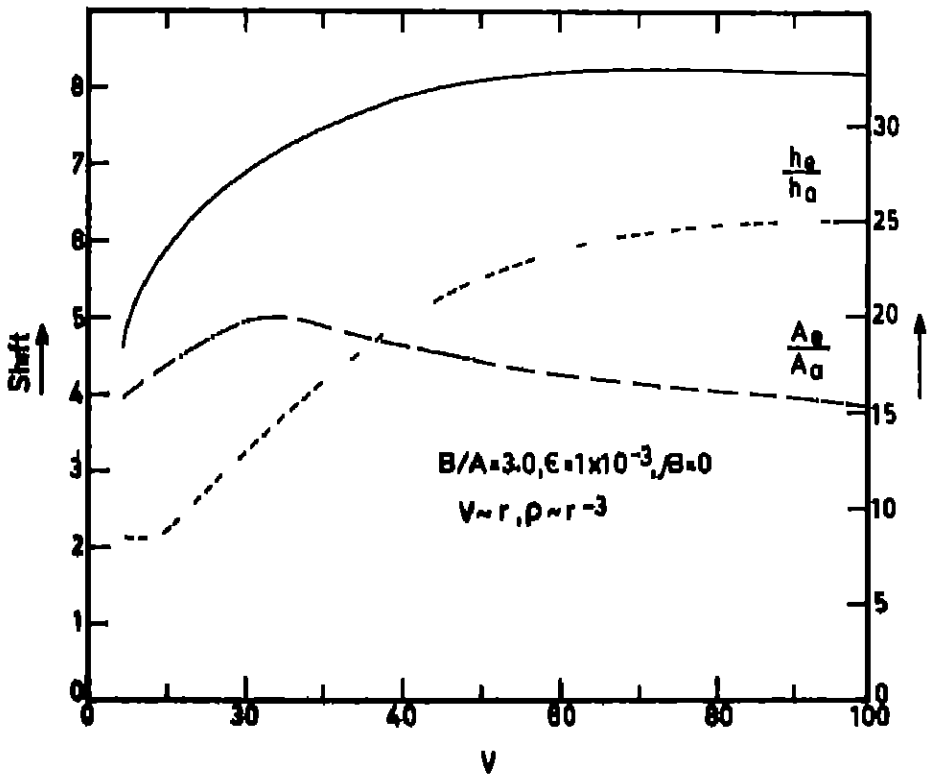

Fig.23a h_e/h_c and A_e/A_c and the shifts correspond to the profile shown in Figure 23

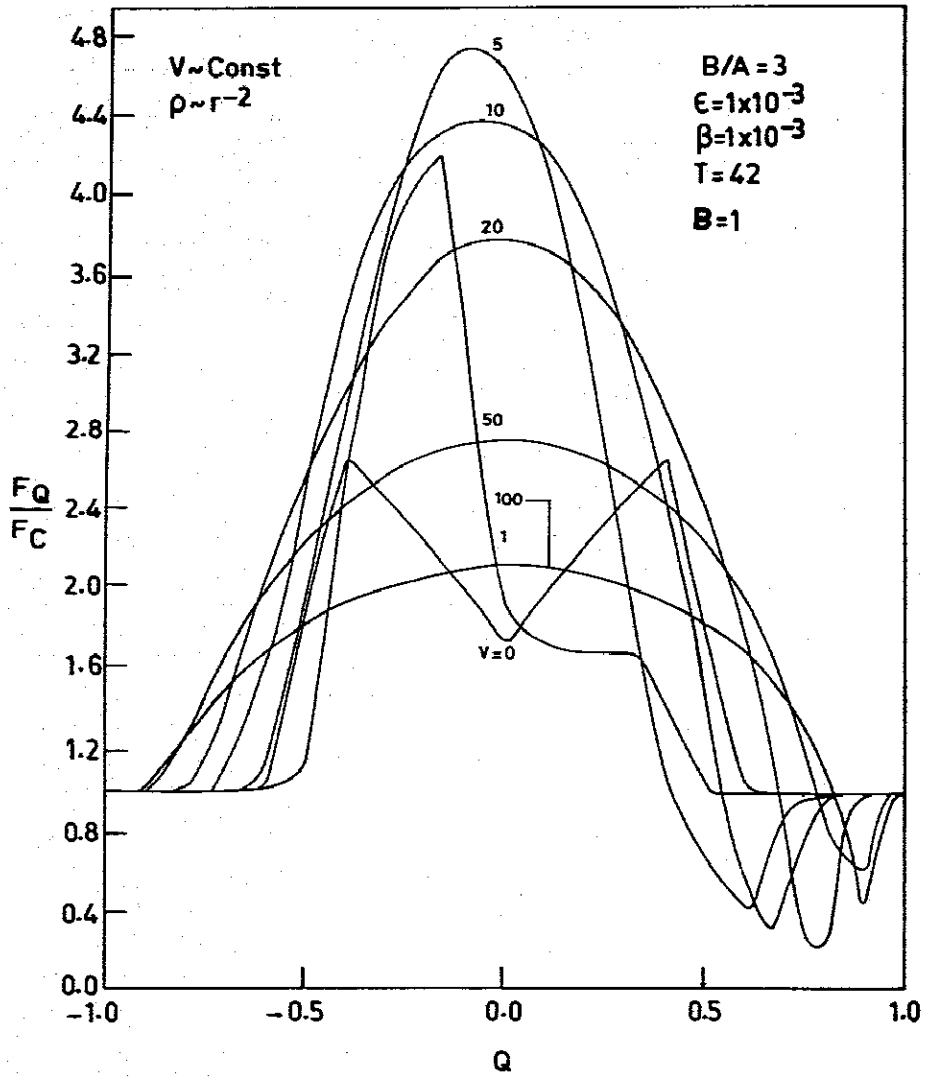

Fig.24 Line profiles with $4\pi r^2 B(r) = 1$

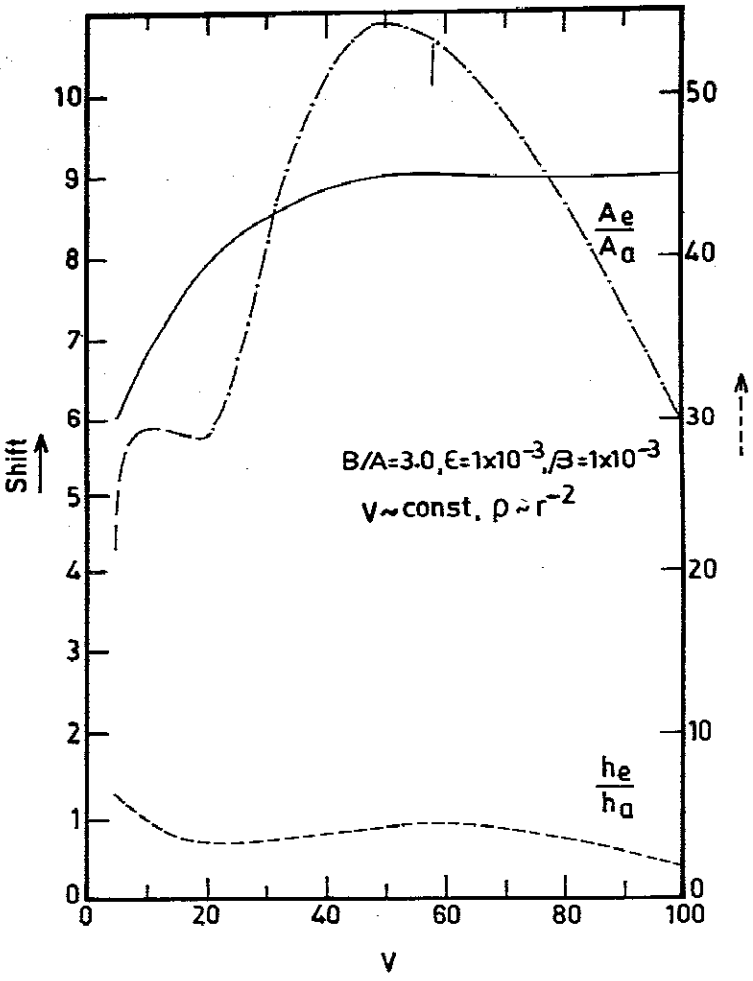

Fig.24a h_e/h_a and A_e/A_a and the shifts correspond to the profile shown in Figure 24

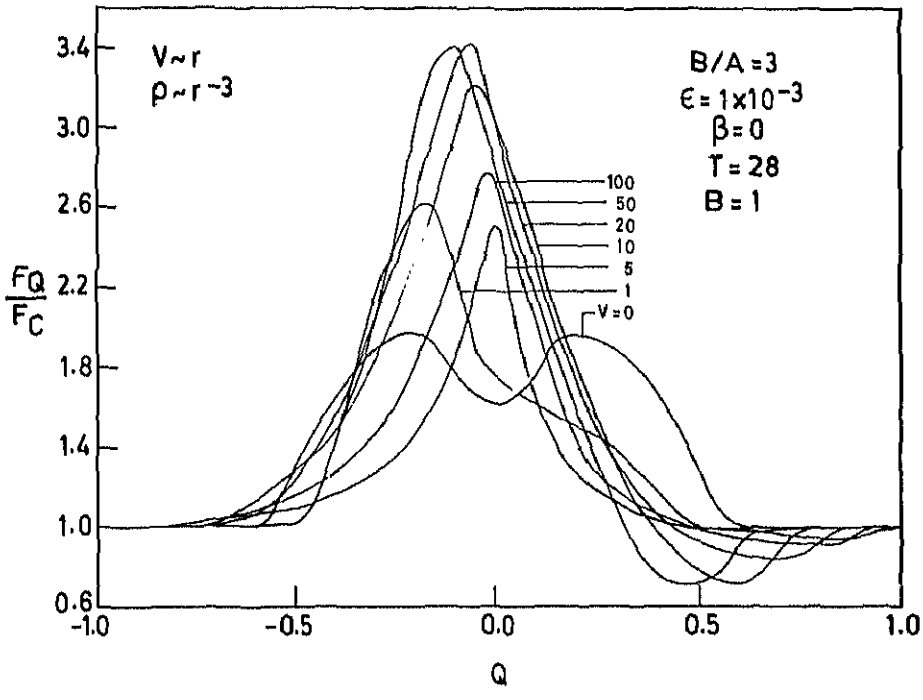

Fig.25 Line profiles with $4\pi r^2 B(r) = 1$

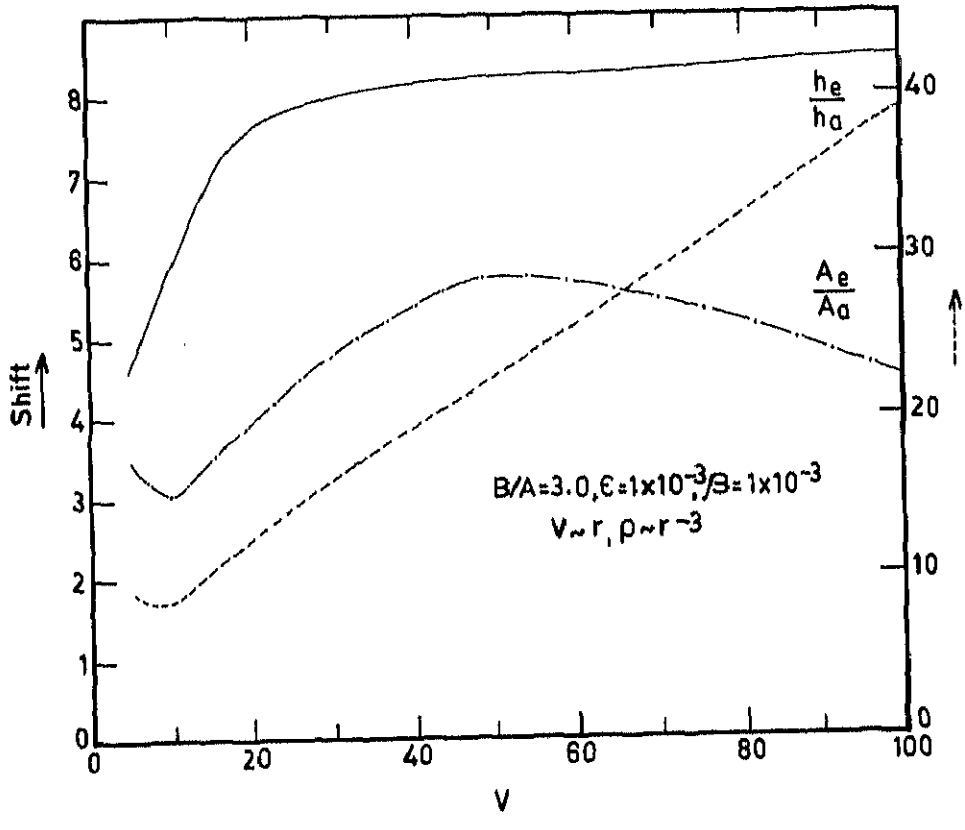

Fig.25a h_e/h_a and A_e/A_a and the shifts correspond to the profile shown in Figure 25

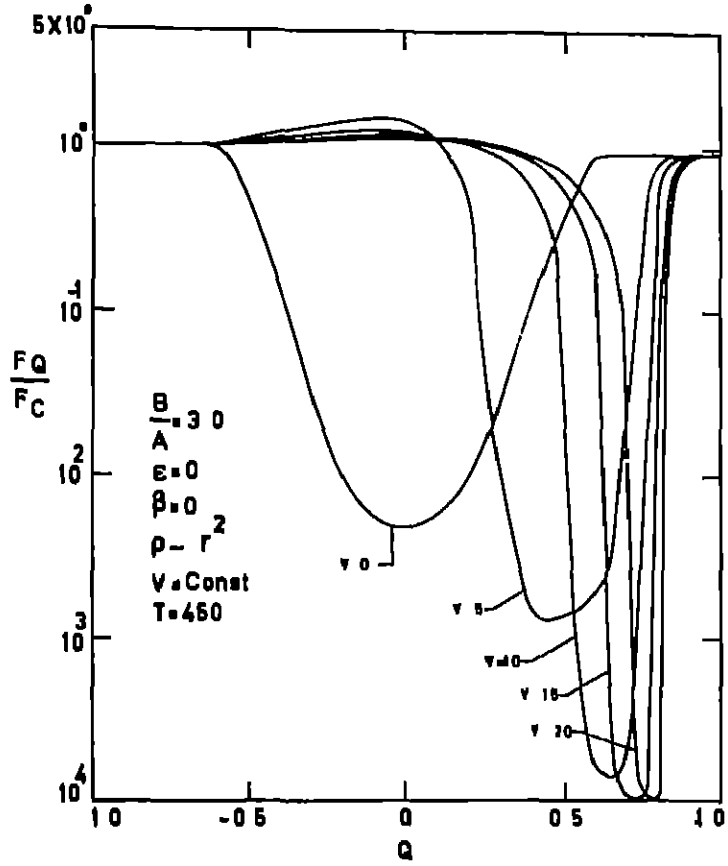

Fig 26 Line profiles.

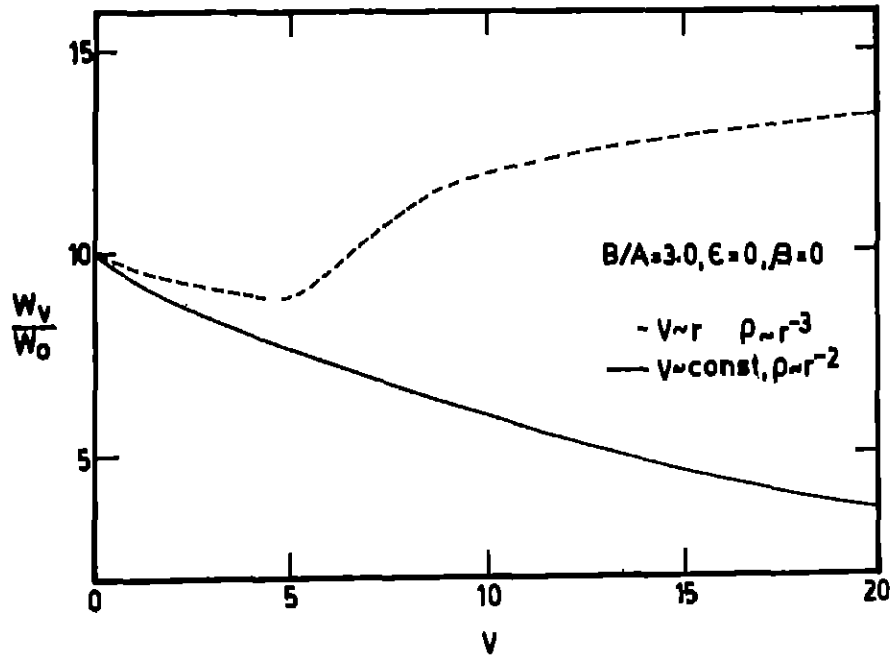

Fig 26a h_e/h_s and A_e/A_s and the shifts correspond to the profile shown in Figure 26

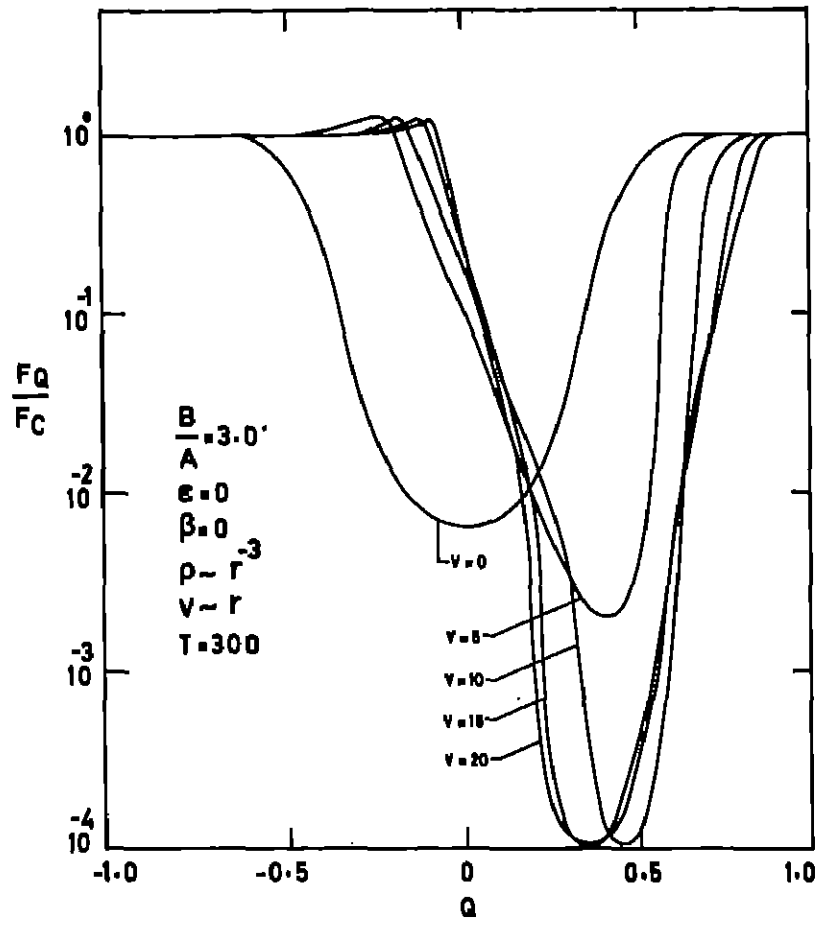

Fig.27 Line profiles.

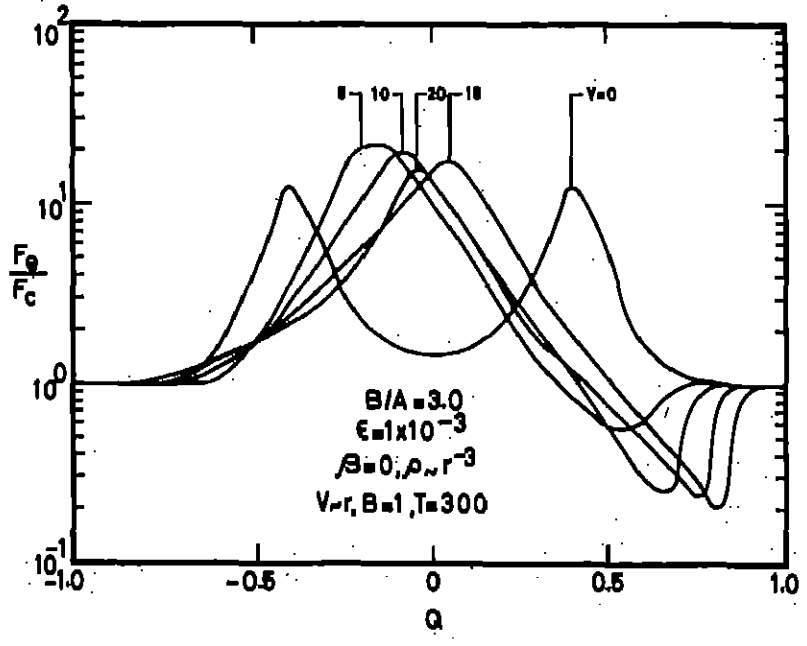

Fig.28 Line profiles with $4\pi r^2 B(r) = 1$.

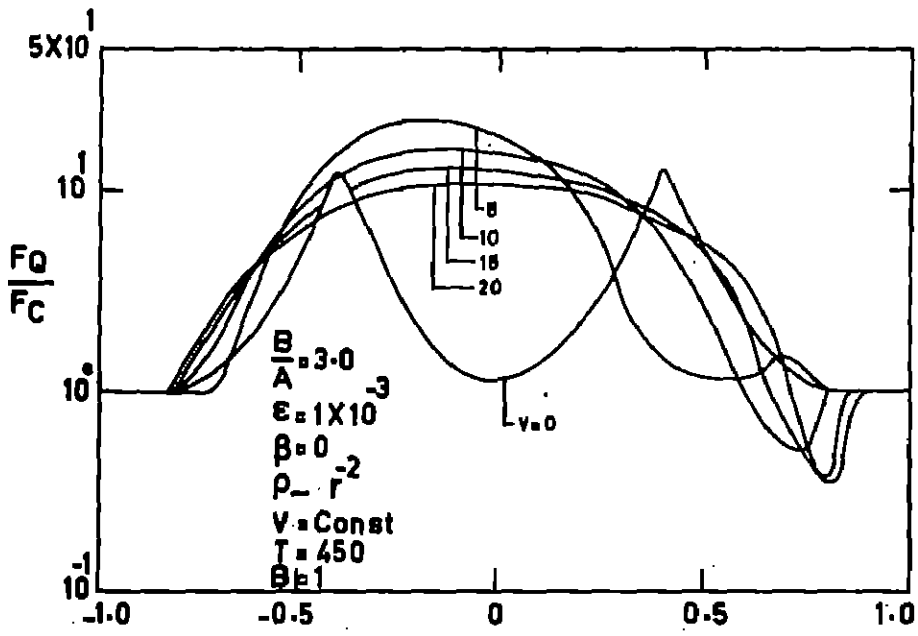

Fig.29 Line profiles with $4\pi r^2 B(r) = 1$

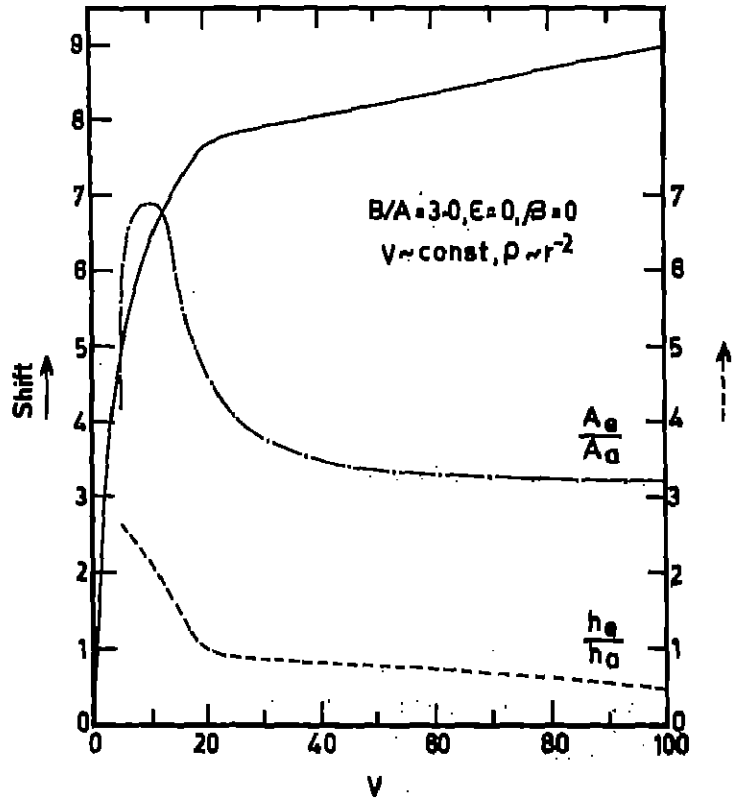

Fig.30 The quantities h_e/h_a and A_e/A_a and shifts are given for parametres shown in the figure.

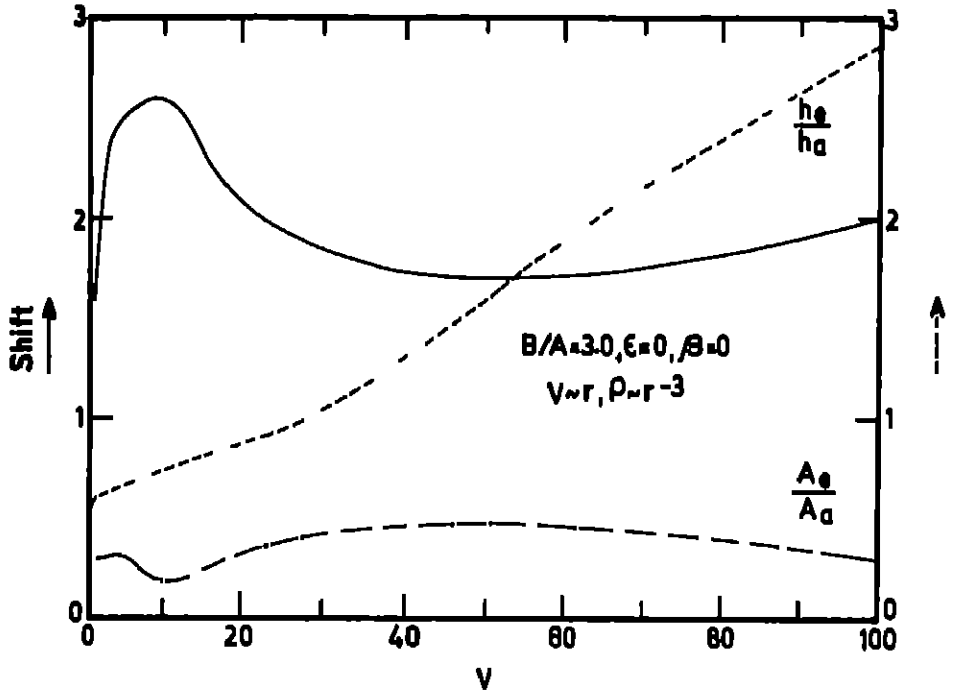

Fig.31 The quantities h_e/h_a and A_e/A_a and shifts are given for parametres shown in the figure.

Conclusions

The method of solving the radiative transfer equation in spherical symmetry described in paper I, is employed to solve the line problem in comoving frame We obtained P Cygni type profiles when high velocities are employed A direct comparison of these profiles with those observed in actual stars can be done easily

References

Beals, C.S., 1950, Pub.Dom.Astrophys.Obs.Vol. 9 No.1, p. 1

Hummer, D.G., and Kunasz, P.B., 1974, Mon.Not., R.Astr.Soc., 166, 10

Mihalas,D.,Kunasz, P.B., and Hummer, D.G.1975, Astrophys. J., 202, 465

Peraiah, A., 1978, Kodaikanal Obs. Bull Ser A, 2, 115

Peraiah, A., 1980a, Acta Astr 30, 523

Peraiah, A., 1980b, J.Astrophys. Astr 1, 3

Peraiah, A., 1984, *In* Methods in Radiative Transfer, ed. W.Kalkofen, Cambridge University Press, p. 281

Peraiah, A., and Varghese, B.A. 1985, Astrophys. J., 290, 411 (Paper 1)

Peraiah, A., and Wehrse, R., 1978, Astr Astrophys., 70, 213

Simmonneau, E. 1973, Astr Astrophys., 29, 357

Wehrse, R., Peraiah, A., 1979, Astr Astrophys., 71, 289

Appendix I

$$A_a = -\alpha - \beta + \gamma + \delta + \rho - \sigma - \varepsilon + \lambda$$

$$A_b = -\alpha + \beta - \gamma + \delta + \rho - \sigma + \varepsilon - \lambda$$

$$A_c = -\alpha + \beta - \gamma + \delta - \rho + \sigma - \varepsilon + \lambda$$

$$A_d = -\alpha - \beta + \gamma + \delta - \rho + \sigma + \varepsilon - \lambda$$

$$A_e = \alpha - \beta - \gamma + \delta - \rho - \sigma + \varepsilon + \lambda$$

$$A_f = \alpha - \beta - \gamma + \delta + \rho + \sigma - \varepsilon - \lambda$$

$$A_g = \alpha + \beta + \gamma + \delta + \rho + \sigma + \varepsilon + \lambda$$

$$A_h = \alpha + \beta + \gamma + \delta - \rho - \sigma - \varepsilon - \lambda$$

$$A'_a = -\alpha' - \beta' + \gamma' + \delta' + \rho - \sigma - \varepsilon + \lambda$$

$$A'_b = -\alpha' + \beta' - \gamma' + \delta' + \rho - \sigma + \varepsilon - \lambda$$

$$A'_c = -\alpha' + \beta' - \gamma' + \delta' - \rho + \sigma - \varepsilon + \lambda$$

$$A'_d = -\alpha' - \beta' + \gamma' + \delta' - \rho + \sigma + \varepsilon - \lambda$$

$$A'_e = \alpha' - \beta' - \gamma' + \delta' - \rho - \sigma + \varepsilon + \lambda$$

$$A'_f = \alpha' - \beta' - \gamma' + \delta' + \rho + \sigma - \varepsilon - \lambda$$

$$A'_g = \alpha' + \beta' + \gamma' + \delta' + \rho + \sigma + \varepsilon + \lambda$$

$$A'_h = \alpha' + \beta' + \gamma' + \delta' - \rho - \sigma - \varepsilon - \lambda$$

Appendix II

$$\alpha = \frac{1}{6}\tau_x \frac{\Delta A}{\bar{A}} - 2\bar{\mu}\left(1 - \frac{\bar{r}}{\Delta r}\frac{\Delta A}{\bar{A}}\right)$$

$$\beta = \frac{\Delta A}{\bar{A}}\left(\frac{1-\bar{\mu}^2}{\Delta\mu} - \frac{1}{6}\Delta\mu\right)$$

$$\gamma = \frac{1}{3}\Delta\mu\left(\frac{\bar{r}}{\Delta r}\frac{\Delta A}{\bar{A}} - 1\right) + \frac{2}{\Delta\mu}(1-\bar{\mu}^2)\left(2 - \frac{\bar{r}}{\Delta r}\frac{\Delta A}{\bar{A}}\right)$$

$$\delta = \tau_x - \bar{\mu}\frac{\Delta A}{\bar{A}}$$

$$\rho = \frac{2}{\Delta x}\left\{\frac{1}{2}V'(1-\bar{\mu}^2)\frac{\Delta A}{\bar{A}} + \bar{\mu}^2\Delta V'\right\}$$

$$\sigma = \frac{2}{\Delta x}\left\{V'(1-\bar{\mu}^2)\left(2 - \frac{\bar{r}}{\Delta r}\frac{\Delta A}{\bar{A}}\right) + \frac{1}{6}\Delta V'\,\bar{\mu}^2\frac{\Delta A}{\bar{A}}\right\}$$

$$\epsilon = \frac{2}{\Delta x}\left\{\frac{1}{3}\Delta\mu\bar{\mu}\left[\left(\Delta V' - \tfrac{1}{2}V'\frac{\Delta A}{\bar{A}}\right)\right]\right\}$$

$$\lambda = \frac{2}{\Delta x}\left\{\frac{1}{3}\Delta\mu\bar{\mu}\left[\frac{1}{6}\Delta V'\frac{\Delta A}{\bar{A}} - V'\left(2 - \frac{\bar{r}}{\Delta r}\frac{\Delta A}{\bar{A}}\right)\right]\right\}$$

$$\alpha' = \frac{1}{6}\tau_x \frac{\Delta A}{\bar{A}} + 2\bar{\mu}\left(1 - \frac{\bar{r}}{\Delta r}\frac{\Delta A}{\bar{A}}\right)$$

$$\beta' = \frac{\Delta A}{\bar{A}}\left(\frac{1}{6}\Delta\mu - \frac{1-\bar{\mu}^2}{\Delta\mu}\right)$$

$$\gamma' = \frac{1}{3}\Delta\mu\left(1 - \frac{\bar{r}}{\Delta r}\frac{\Delta A}{\bar{A}}\right) + \frac{2}{\Delta\mu}(1-\bar{\mu}^2)\left(\frac{\bar{r}}{\Delta r}\frac{\Delta A}{\bar{A}} - 2\right)$$

$$\delta' = \tau_x + \bar{\mu}\frac{\Delta A}{\bar{A}}$$

$$\tau_x = \tau\,\phi(x)$$